

This is the accepted manuscript made available via CHORUS. The article has been published as:

Random walks with thermalizing collisions in bounded regions: Physical applications valid from the ballistic to diffusive regimes

C. M. Swank, A. K. Petukhov, and R. Golub

Phys. Rev. A **93**, 062703 — Published 8 June 2016

DOI: [10.1103/PhysRevA.93.062703](https://doi.org/10.1103/PhysRevA.93.062703)

Random walks with thermalizing collisions in bounded regions; physical applications valid from the ballistic to diffusive regimes.

C.M. Swank,¹ A.K. Petukhov,² and R. Golub³

¹*Division of Physics, Math and Astronomy, California Institute of Technology, Pasadena, CA*

²*Institut Laue-Langevin, BP156, 38042 Grenoble Cedex 9, France*

³*Physics Department, North Carolina State University, Raleigh, NC 27695*

The behavior of a spin undergoing Larmor precession in the presence of fluctuating fields is of interest to workers in many fields. The fluctuating fields cause frequency shifts and relaxation which are related to their power spectrum, which can be determined by taking the Fourier transform of the auto-correlation functions of the field fluctuations. Recently we have shown how to calculate these correlation functions for all values of mean free path (ballistic to diffusive motion) in finite bounded regions, using the model of persistent continuous time random walks (CTRW) for particles subject to scattering by fixed (frozen) scattering centers so that the speed of the moving particles is not changed by the collisions. In this work we show how scattering with energy exchange from an ensemble of scatterers in thermal equilibrium can be incorporated into the CTRW. We present results for 1,2 and 3 dimensions. The results agree for all these cases contrary to the previously studied 'frozen' models. Our results for the velocity autocorrelation function show a long time tail ($\sim t^{-1/2}$), which we also obtain from conventional diffusion theory, with the same power, independent of dimensionality.

Our results are valid for any Markovian scattering kernel as well as any kernel based on a scattering cross section $\sim 1/v$.

I. INTRODUCTION

The dynamics of a system of spins moving under the influence of static and time-varying magnetic fields is a subject of wide ranging scientific and technical interest. Both randomly fluctuating fields produced by a thermal reservoir, and fluctuations seen by particles undergoing stochastic trajectories in inhomogeneous fields have been the subject of intense study over many decades. It was Bloembergen, Purcell and Pound¹ who first showed, using physical arguments based on Fermi's golden rule, that the relaxation rate is determined by the power spectrum of the fluctuating fields evaluated at the Larmor frequency. In general power spectra of fluctuating quantities are given by the Fourier transform of the auto-correlation of the fluctuating variable. A short history of the development of the field can be found in the introductions to^{2,3}.

One of the applications of these techniques is to the next generation searches for a particle electric dipole moment(EDM) which require measurements of spin dynamics in uniform magnetic fields with nanohertz precision. Furthermore, searches for fundamental forces beyond the standard model require similar accuracy in the measurement of Longitudinal and Transverse relaxation (T_1 and T_2) expected to be produced by the hypothesized interaction. The desire for such accurate predictions inspires the search for models of particle trajectories in the case of particles moving in inhomogeneous fields.

Redfield⁴, as elucidated by Slichter⁵, and McGregor⁶ have given formal derivations of the relation between relaxation and the autocorrelation functions of the fields and the method was applied to a 'false edm' systematic error effecting searches for time reversal and parity violating non-zero particle electric dipole moments^{7,8}. General methods for obtaining auto-correlation functions for fluctuations produced by particles diffusing in inhomogeneous fields with arbitrary spatial variation have been given by⁹ and¹⁰.

This work has been extended by¹¹ to the case of arbitrary field variation and all values of scattering mean free path (from ballistic to diffusive motion) in restricted geometries. The method used was based on the persistent continuous time random walk model of Masoliver et

al,¹², who solved a transport equation for the Laplace-Fourier transform of the conditional probability $P(\vec{r}, t)$ (the probability that a particle located at $\vec{r} = 0$ at $t = 0$, will be found at position \vec{r} at time t (sometimes called a propagator), for the case of an infinite domain. The model assumed a collection of fixed scattering centers ('frozen' environment) so that the speed of the particles was unchanged by the scattering events, and was valid for all values of the mean free path. The authors of¹¹ applied the results of Masoliver et al,¹² to 2 and 3 dimensional regions bounded by rectangles, by using the method of images and used the resulting conditional probabilities to calculate a number of spectra of autocorrelation functions relevant to relaxation and frequency shifts in a range of problems. See³ for an overview of the relation between correlation functions of fluctuating fields and physical phenomena.

In references^{13,14} the authors used a similar method to derive the propagator, conditional probability for one dimensions, in the presence of an external force, for example gravity, in the asymptotic limit of small spacial and temporal frequencies.

In the present work we apply the technique of Swank et al¹¹ to the case of Markovian scattering in which each collision completely re-thermalizes the scattered particles. The method applies equally to the case when the total inelastic scattering cross section $\sim 1/v$ with v the particle velocity. We find that the results differ somewhat from those obtained by averaging the results for the frozen environment over the velocity distribution of the scattered particles and that the results for 1, 2 and 3 dimensions are identical when averaged over a Maxwell distribution. Further we show that for stochastic bounded motion the velocity autocorrelation functions have long time tails proportional to $t^{-1/2}$, in all cases where diffusion theory is valid, in agreement with the one dimensional treatment in reference¹⁵. Other studies have shown that in non-bounded systems long-range hydrodynamic forces lead to different results ($\sim t^{-d/2}$) where d is the number of dimensions of the system. We present the results of applying our method to the physically interesting problems of the false edm systematic error in searches for particle electric dipole moments and to calculating the position and velocity autocorrelation functions for particles confined to a bounded region, which determine

frequency shifts and relaxation rates in nmr,³.

II. THE MODEL

A. Preliminaries: Persistent continuous time random walk in the frozen environment.

In this section we review the solution for the spectrum of the probability density of a persistent continuous time random walk (CTRW) as presented in the work of Weiss and co-workers¹². The particles are assumed to travel ballistically with fixed velocity v between scattering events. The time between scattering events is governed by a distribution $\psi(t)$, such that the probability to scatter within a time segment dt is given by $\psi(t)dt$, and the probability to reach t without scattering is given by $\Psi(t) = \int_t^\infty \psi(t)dt$. The conditional probability $p(\mathbf{x}, t)$, is calculated, as well as a scattering density $\rho(\mathbf{x}, t)$, the probability of scattering at \mathbf{x} and time t . A recursive equation that completely describes the CTRW is formed for the two densities,

$$\begin{aligned} \rho(\mathbf{x}, t, v, \Omega) = & f(\mathbf{x}, t, v) \alpha(\Omega) \psi(t) \\ & + \int \int \int d^3 \mathbf{x}' dt' d\Omega' f(\mathbf{x} - \mathbf{x}', t - t', v) \beta(\Omega | \Omega') \psi(t - t') \int dv' \rho(\mathbf{x}', t', v'), \\ p(\mathbf{x}, t, v, \Omega) = & f(\mathbf{x}, t, v) \alpha(\Omega) \Psi(t) \end{aligned} \quad (1)$$

$$+ \int \int \int d^3 \mathbf{x}' dt' d\Omega' f(\mathbf{x} - \mathbf{x}', t - t', v) \beta(\Omega | \Omega') \Psi(t - t') \int dv' \rho(\mathbf{x}', t', v'), \quad (2)$$

In three dimensions the angular coordinates denoted by $\Omega = \{\theta, \phi\}$ has element $d\Omega = \sin\theta d\theta d\phi$. $\alpha(\Omega)$ is the initial angular density, while $\beta(\Omega | \Omega')$ is the conditional angular density having scattered from a previous angle Ω' also known as the scattering kernel. We will assume the initial angular density to be isotropic and the angular conditional density to be isotropic

and Markovian. Therefore in three dimensions we have,

$$\alpha(\Omega) = \beta(\Omega|\Omega') = \frac{1}{4\pi}.$$

In three dimensions $f(\mathbf{x}, t, v)$ is given by,

$$f(\mathbf{x}, t, v) = \delta(x - vt \sin \theta \cos \phi) \delta(y - vt \sin \theta \sin \phi) \delta(z - vt \cos \theta). \quad (3)$$

The scattering time density will be assumed to follow a simple Poisson distribution:

$$\psi(t) = \frac{1}{\tau_c} e^{-\frac{t}{\tau_c}}. \quad (4)$$

where τ_c is the average collision time. The spectrum of the conditional density is found by applying the Laplace-Fourier Transform to equations (2)¹²:

$$p(\mathbf{q}, s) = \tau_c \frac{\arctan\left(\frac{qv\tau_c}{1+s\tau_c}\right)}{qv\tau_c - \arctan\left(\frac{qv\tau_c}{1+s\tau_c}\right)}. \quad (5)$$

In our previous work¹¹, we extended the free space solution shown in equation (5) (for the 3D case) to the restricted domain in 1, 2 and 3 dimensions. In the present work we allow the velocity to change upon a scattering event, changing the model from a "frozen" model with fixed speed, to one that allows momentum transfer. The approach is similar to that shown in reference¹⁶. We will see that the result differs from simply averaging the single velocity conditional density over velocity and that the results for three dimensions are identical to the results for lower dimensions, and a method for predicting three dimensional results from a one dimensional model (in Cartesian coordinates) is obtained. Results for the position and velocity autocorrelation functions and applications to the bounded domain are presented.

B. From the frozen environment to thermalization with momentum transfer.

In the following we present our model of a CTRW with thermalization that we refer to as CTRWT. We start from the approach described above,¹². A change in velocity upon a

gas scattering can be accounted for by including a probability distribution for the outgoing velocity after a scattering event. The treatment of v is identical to that of reference¹² for the angular density, except now we allow the vector velocity \mathbf{v} to change. Therefore we extend functions $\alpha(\Omega)$ and $\beta(\Omega|\Omega') \rightarrow \alpha(\mathbf{v})$ and $\beta(\mathbf{v}|\mathbf{v}')$. Now $\alpha(\mathbf{v})$ is the initial probability distribution of velocities with angle Ω and speed v and $\beta(\mathbf{v}|\mathbf{v}')$ is the probability of scattering into angle Ω and speed v with incoming angle Ω' and speed v' prior to the collision,

$$\rho(\mathbf{x}, t, \mathbf{v}) = f(\mathbf{x}, t, \mathbf{v})\alpha(\mathbf{v})\psi(t) + \int d^3\mathbf{x}' dt' f(\mathbf{x} - \mathbf{x}', t - t', \mathbf{v})\psi(t - t') \int d^3\mathbf{v}' \beta(\mathbf{v}|\mathbf{v}')\rho(\mathbf{x}', t', \mathbf{v}'). \quad (6)$$

Where $f(\mathbf{x}, t, \mathbf{v})$ is given by,

$$f(\mathbf{x}, t, \mathbf{v}) = \delta^{(N)}(\mathbf{x} - \mathbf{v}t), \quad (7)$$

for N dimensions. This is similar to the formulation in¹⁶, where they derive the spectrum of the conditional density and correlation functions in one dimension for arbitrary scattering time densities.

Now the scattering density,

$$\rho(\mathbf{x}', t', \mathbf{v}') = N_s \sigma_{tot}(v') v' n(\mathbf{x}', t', \mathbf{v}'), \quad (8)$$

where N_s is the number of scatterers per unit volume, $\sigma_{tot}(v')$ is the total inelastic scattering cross section and $n(\mathbf{x}', t', \mathbf{v}')$ is the density of particles with velocity v' at (\mathbf{x}', t') . The double differential cross section $\sigma(\mathbf{v}' \rightarrow \mathbf{v}) = \beta(\mathbf{v}|\mathbf{v}')\sigma_{tot}(v')$.

For a system in thermal equilibrium:

$$n(\mathbf{x}', t', \mathbf{v}') = \alpha(\mathbf{v}') n(\mathbf{x}', t'). \quad (9)$$

For the common case $\sigma_{tot}(v') \propto 1/v'$, we can write,

$$\rho(\mathbf{x}', t', \mathbf{v}') = \alpha(\mathbf{v}') \rho(\mathbf{x}', t'), \quad (10)$$

where $\rho(\mathbf{x}', t') = N_s \sigma_{tot}(v') v' n(\mathbf{x}', t')$ is then independent of v' .

Thus the second term in (6) becomes,

$$\begin{aligned} & \int d^3\mathbf{x}' dt' f(\mathbf{x} - \mathbf{x}', t - t', \mathbf{v}) \psi(t - t') \int d^3\mathbf{v}' \beta(\mathbf{v}|\mathbf{v}') \alpha(\mathbf{v}') \rho(\mathbf{x}', t') \\ &= \alpha(\mathbf{v}) \int d^3\mathbf{x}' dt' f(\mathbf{x} - \mathbf{x}', t - t', \mathbf{v}) \psi(t - t') \rho(\mathbf{x}', t'), \end{aligned} \quad (11)$$

making use of the property,

$$\int d^3\mathbf{v}' \beta(\mathbf{v}|\mathbf{v}') \alpha(\mathbf{v}') = \alpha(\mathbf{v}), \quad (12)$$

which must be satisfied by any physically allowable kernel that produces a Maxwellian steady state. Thus our method is valid for a variety of experimentally relevant collision kernels such as the cusp kernels introduced in¹⁷. For a Markovian thermalization process $\beta(\mathbf{v}|\mathbf{v}') = \alpha(\mathbf{v})$ independent of \mathbf{v}' and (11) follows directly from equation (6).

With this included our transport equations become,

$$\rho(\mathbf{x}, t, \mathbf{v}) = \alpha(\mathbf{v}) f(\mathbf{x}, t, \mathbf{v}) \psi(t) + \alpha(\mathbf{v}) \int d^3\mathbf{x}' dt' f(\mathbf{x} - \mathbf{x}', t - t', \mathbf{v}) \psi(t - t') \rho(\mathbf{x}', t'), \quad (13)$$

$$p(\mathbf{x}, t, \mathbf{v}) = \alpha(\mathbf{v}) f(\mathbf{x}, t, \mathbf{v}) \Psi(t) + \alpha(\mathbf{v}) \int d^3\mathbf{x}' dt' f(\mathbf{x} - \mathbf{x}', t - t', \mathbf{v}) \Psi(t - t') \rho(\mathbf{x}', t'). \quad (14)$$

The remarkable property of our model (13, 14) is that it is independent of the form of the scattering kernel as long as (12) is satisfied.

Since we are mainly interested in finding the velocity averaged probability, $p(\mathbf{q}, s)$, We introduce the velocity integrated quantities,

$$p(\mathbf{x}, t) = \int p(\mathbf{x}, t, \mathbf{v}) d^3\mathbf{v}, \quad (15)$$

$$\rho(\mathbf{x}, t) = \int \rho(\mathbf{x}, t, \mathbf{v}) d^3\mathbf{v}. \quad (16)$$

The first term in equation (13) represents all of the particles that make their first scattering at (\mathbf{x}, t) . The second term, a convolution of the f propagator and scattering density ρ

represents particles that have scattered at (\mathbf{x}', t') and traveled to (\mathbf{x}, t) where they make another collision. From here they can make another collision (13) or continue on the same path without scattering, but they contribute to the particle density at (\mathbf{x}, t) (14).

We will take advantage of the convolution theorem of the Fourier-Laplace transform to solve for the spectrum, $p(\mathbf{q}, s)$. Setting,

$$g(\mathbf{x} - \mathbf{x}', t - t', \mathbf{v}) = f(\mathbf{x} - \mathbf{x}', t - t', \mathbf{v})\psi(t - t'), \quad (17)$$

$$G(\mathbf{x} - \mathbf{x}', t - t', \mathbf{v}) = f(\mathbf{x} - \mathbf{x}', t - t', \mathbf{v})\Psi(t - t'),$$

we have from (13),

$$\rho(\mathbf{q}, s, \mathbf{v}) = \alpha(\mathbf{v})g(\mathbf{q}, s, \mathbf{v}) + \rho(\mathbf{q}, s)\alpha(\mathbf{v})g(\mathbf{q}, s, \mathbf{v}), \quad (18)$$

$$p(\mathbf{q}, s, \mathbf{v}) = \alpha(\mathbf{v})G(\mathbf{q}, s, \mathbf{v}) + \rho(\mathbf{q}, s)\alpha(\mathbf{v})G(\mathbf{q}, s, \mathbf{v}), \quad (19)$$

so that,

$$p(\mathbf{q}, s) = \frac{\int \alpha(\mathbf{v})G(\mathbf{q}, s, \mathbf{v})d^3\mathbf{v}}{1 - \int \alpha(\mathbf{v})g(\mathbf{q}, s, \mathbf{v})d^3\mathbf{v}}. \quad (20)$$

For gas collisions that randomize velocity after each collision the correct conditional probability density, p , is not a direct velocity average of the single velocity p , but a function of the velocity average of the individual propagators of G and g .

The collision time and the probability of scattering $\psi(t)$ remain the same for all three dimensions,

$$\psi(t) = \frac{1}{\tau_c}e^{-\frac{1}{\tau_c}t}, \quad (21)$$

where $\frac{1}{\tau_c}$ is the rate of gas collisions. The probability of not making a scattering in time t is given by the integration over the scattering rate,

$$\Psi(t) = \int_t^\infty \psi(t)dt = e^{-\frac{t}{\tau_c}}. \quad (22)$$

We define:

$$F_N(\mathbf{x}, t) = \int \alpha_N(\mathbf{v}) G_N(\mathbf{x}, t, \mathbf{v}) d^N \mathbf{v}, \quad (23)$$

where N represents the number of dimensions in the random walk. We now find the Fourier-Laplace transform of $F_N(\mathbf{x}, t)$,

$$F_N(\mathbf{q}, s) = \int_0^\infty dt \int \alpha_N(\mathbf{v}) \delta^{(N)}(\mathbf{x} - \mathbf{v}t) e^{-\frac{t}{\tau_c} - i\mathbf{q} \cdot \mathbf{x} - st} d^N \mathbf{x} d^N \mathbf{v}. \quad (24)$$

We will use the Maxwellian velocity distribution:

$$\alpha_N(\mathbf{v}) = \prod_{i=1}^N \left(\frac{1}{2} \sqrt{\frac{2m}{\pi kT}} \right) e^{-\frac{m}{2kT} v_i^2}. \quad (25)$$

Substituting this into equation (24),

$$F_N(\mathbf{q}, s) = \int_0^\infty dt \int \left[\prod_{i=1}^N \left(\frac{1}{2} \sqrt{\frac{2m}{\pi kT}} \right) e^{-\frac{m}{2kT} v_i^2} \right] \delta^{(N)}(\mathbf{x} - \mathbf{v}t) e^{-\frac{t}{\tau_c} - i\mathbf{q} \cdot \mathbf{x} - st} d^N \mathbf{x} d^N \mathbf{v}, \quad (26)$$

and integration over position gives

$$F_N(\mathbf{q}, s) = \int_0^\infty dt e^{-(s + \frac{1}{\tau_c})t} \prod_{i=1}^N \left(\frac{1}{2} \sqrt{\frac{2m}{\pi kT}} \right) \int e^{-\frac{m}{2kT} v_i^2 - i q_i v_i t} dv_i, \quad (27)$$

integration over v_i then gives,

$$F_N(\mathbf{q}, s) = \int_0^\infty dt e^{-(s + \frac{1}{\tau_c})t} \prod_{i=1}^N e^{-\frac{1}{2} \frac{kT}{m} t^2 q_i^2}, \quad (28)$$

$$= \int_0^\infty dt e^{-(s + \frac{1}{\tau_c})t - \frac{1}{2} \frac{kT}{m} t^2 q^2}. \quad (29)$$

Finally performing the Laplace transform we find,

$$\begin{aligned} F_N(\mathbf{q}, s) &= \sqrt{\frac{\pi m}{2kT q^2}} e^{\frac{m}{2kT} \frac{(s + \frac{1}{\tau_c})^2}{q^2}} \operatorname{erfc} \left(\sqrt{\frac{m}{2kT}} \frac{s + \frac{1}{\tau_c}}{q} \right), \\ &= \sqrt{\frac{\pi m}{2kT q^2}} e^{z^2} \operatorname{erfc}(z) \equiv F(q, z), \end{aligned} \quad (30)$$

where,

$$z(q, s) = \sqrt{\frac{m}{2kT}} \frac{1}{\tau_c} \frac{(1 + s\tau_c)}{q}. \quad (31)$$

We have been working with the Laplace transform of various functions of time. This implies that these functions are causal i.e. equal to zero for $t < 0$. If we make the replacement $s \rightarrow i\omega$, and take two times the real part of the resulting expression, the results will apply to the even ($f(-t) = f(t)$) extension of the causal functions in agreement with other authors e.g.⁶. Unless specified it should be assumed that a spectrum refers to the even extension. From now on we use,

$$F(q, \omega) = F(q, z(q, s = i\omega)). \quad (32)$$

It is immediately seen that the result is independent of the number of dimensions N . The dimensionality of the model only appears in q where,

$$q^2 = \sum_{i=1}^N q_i^2.$$

We note that q can never be negative, this is important to remember when integrating and/or summing over discrete values of q . However, q_i , a single component of \mathbf{q} can be negative. The conditional density for any number of dimensions (20) can be written as,

$$p(q, \omega) = 2 \operatorname{Re} \left[\frac{F(q, \omega)}{1 - \frac{1}{\tau_c} F(q, \omega)} \right]. \quad (33)$$

Thus, we observe agreement for the spectrum of the conditional probability given by the CTRWT for 1, 2, and 3 dimensions. Furthermore, there are no cross correlations between the different directions in Cartesian coordinates, therefore one can compute values of a higher dimensional model from a lower dimensional model, given that this model was projected from Cartesian coordinates. Assuming Cartesian coordinates and given no cross-correlation in the components of the functions being correlated we can compute a 3D result from three 1D results, or one 2D result and one 1D result. In the latter case the 2D model can include functions with cross correlation.

1. *Comparison with diffusion theory.*

To compare to diffusion theory we define a length scale and ballistic collision time, naturally the ballistic time should scale linearly with the length, and inversely with the thermal speed of the system, thus $\tau_b = L\sqrt{\frac{m}{kT}}$. For diffusion theory to be valid we must have $\tau_b/\tau_c \gg 1$ and $1 \gg \omega\tau_c$ so that z becomes very large for not too large q ,

$$z \approx \sqrt{\frac{m}{2kT}} \frac{1}{\tau_c} \frac{1}{q} = \frac{1}{\sqrt{2}} \frac{\tau_b}{\tau_c} \frac{1}{qL_x} \gg 1.$$

For large z the asymptotic expansion for the complimentary error function can be used,

$$\text{erfc}(z) \rightarrow \frac{e^{-z^2}}{\sqrt{\pi}z} \left(1 - \frac{1}{2z^2}\right). \quad (34)$$

For now, we keep the full form of z prior to expansion of the error function, and substitute equation (34) into equation (33),

$$p(q, s = i\omega) = 2 \text{Re} \left(\frac{(1 + i\omega\tau_c)^2}{\frac{kT}{m}q^2\tau_c + i\omega(1 + i\omega\tau_c)^2} \right). \quad (35)$$

We then take the diffusion limit ($\omega\tau_c \ll 1$) with the result,

$$p(q, \omega) = 2 \text{Re} \left(\frac{1}{\frac{kT}{m}q^2\tau_c + i\omega} \right) = 2 \text{Re} \left(\frac{1}{(Dq^2) + i\omega} \right). \quad (36)$$

Since $D_N = \frac{\langle v_N^2 \rangle}{N} \tau_c$ where N is the number of dimensions and $\langle v_N^2 \rangle = N \frac{kT}{m}$, we have inserted the diffusion coefficient,

$$D = \tau_c \frac{kT}{m}. \quad (37)$$

Equation (36) is immediately seen to be the Fourier transform of the Green's function of the diffusion equation.

C. Vector velocity autocorrelation function in an infinite domain.

The vector velocity autocorrelation function can be written as an integration over the vector components of velocity, analogous to the one dimensional treatment in ¹⁶,

$$S_{\mathbf{v}\mathbf{v}}(\mathbf{q}, s) = \int_{-\infty}^{\infty} \mathbf{v} \cdot \mathbf{v}_0 p_{\mathbf{v}\mathbf{v}_0}(\mathbf{q}, s) \alpha(\mathbf{v}_0) d^3 \mathbf{v}_0 d^3 \mathbf{v}. \quad (38)$$

Where $p_{\mathbf{v}\mathbf{v}_0}(\mathbf{q}, s)$ is the ¹⁶ Fourier-Laplace transform of the conditional probability for a particle which has velocity \mathbf{v}_o at $(\mathbf{x} = 0, t = 0)$ to have the velocity \mathbf{v} at (\mathbf{x}, t) and satisfies,

$$p_{\mathbf{v}\mathbf{v}_0}(\mathbf{q}, s) = G_v(\mathbf{q}, s) \delta(\mathbf{v} - \mathbf{v}_0) + \alpha(\mathbf{v}) G_v(\mathbf{q}, s) \rho_o(\mathbf{q}, s), \quad (39)$$

where,

$$\rho_o(\mathbf{q}, s) = \frac{g(\mathbf{q}, s, \mathbf{v}_o)}{1 - \int \alpha(\mathbf{v}) g(\mathbf{q}, s, \mathbf{v}) d^3 \mathbf{v}}, \quad (40)$$

is the Laplace-Fourier transform of the scattering density at (\mathbf{x}, t) of particles that started at $(\mathbf{x} = 0, t = 0)$ with velocity \mathbf{v}_o . Then,

$$p_{\mathbf{v}\mathbf{v}_0}(\mathbf{q}, s) = G_v(\mathbf{q}, s) \delta(\mathbf{v} - \mathbf{v}_0) + \frac{\alpha(\mathbf{v}) G_v(\mathbf{q}, s) g(\mathbf{q}, s, \mathbf{v}_o)}{1 - \int \alpha(\mathbf{v}) g(\mathbf{q}, s, \mathbf{v}) d^3 \mathbf{v}}, \quad (41)$$

and using as above, $\frac{1}{\tau_c} G_{\mathbf{v}}(\mathbf{q}, s) = g_{\mathbf{v}}(\mathbf{q}, s)$ we have,

$$S_{\mathbf{v}\mathbf{v}}(\mathbf{q}, s) = \int v^2 G_v(\mathbf{q}, s) \alpha(\mathbf{v}) d^3 \mathbf{v} + \frac{\frac{1}{\tau_c} \left(\int \mathbf{v} \alpha(\mathbf{v}) G_v(\mathbf{q}, s) d^3 \mathbf{v} \right)^2}{1 - \frac{1}{\tau_c} \int \alpha(\mathbf{v}) G_v(\mathbf{q}, s) d^3 \mathbf{v}}. \quad (42)$$

For simplicity we write this equation as

$$S_{\mathbf{v}\mathbf{v}}(\mathbf{q}, s) = H(\mathbf{q}, s) + \frac{\frac{1}{\tau_c} \mathbf{K}(\mathbf{q}, s)^2}{1 - \frac{1}{\tau_c} L(\mathbf{q}, s)}. \quad (43)$$

Where,

$$H(\mathbf{q}, s) = \int v^2 G_v(\mathbf{q}, s) \alpha(\mathbf{v}) d^3\mathbf{v}, \quad (44)$$

$$L(\mathbf{q}, s) = \int G_v(\mathbf{q}, s) \alpha(\mathbf{v}) d^3\mathbf{v}, \quad (45)$$

$$\mathbf{K}(\mathbf{q}, s) = \int \mathbf{v} G_v(\mathbf{q}, s) \alpha(\mathbf{v}) d^3\mathbf{v}, \quad (46)$$

$$G(\mathbf{q}, s) = \frac{1}{\left(s + \frac{1}{\tau_c}\right) + i\mathbf{q} \cdot \mathbf{v}}, \quad (47)$$

Carrying out all the integrations we find:

$$S_{\mathbf{v}\mathbf{v}}(q, s) = \frac{z + \sqrt{\pi} e^{z^2} (1 - z^2) \operatorname{erfc}(z)}{\sqrt{\frac{m}{2kT}} q} - \frac{\lambda \left(\sqrt{\pi} z e^{z^2} \operatorname{erfc}(z) - 1 \right)^2}{q^2 \left(1 - \sqrt{\frac{\pi m}{2kT}} \frac{1}{\tau_c q} e^{z^2} \operatorname{erfc}(z) \right)}. \quad (48)$$

This is the Fourier Laplace transform for the velocity autocorrelation function of an unbounded continuous time random walk in 3D, given a Maxwell velocity distribution, thermalizing gas collisions and Poisson distributed collision times.

To calculate the spectrum of the position averaged velocity autocorrelation function we take the limit as $q \rightarrow 0$, ($z \gg 1$) and we use the asymptotic expansion of the $\operatorname{erfc}(z)$, equation (34), where we must take the expansion to the second term,

$$S_{\mathbf{v}\mathbf{v}}(\omega) = \lim_{q \rightarrow 0} \left(\frac{z + (1 - z^2) \frac{1}{z} (1 - \frac{1}{2z^2})}{\sqrt{\frac{m}{2kT}} q} - \frac{1}{\tau_c q^2} \frac{\left(\frac{1}{2z^2}\right)^2}{1 - \sqrt{\frac{m}{2kT}} \frac{1}{\tau_c q} \frac{1}{z} (1 - \frac{1}{2z^2})} \right). \quad (49)$$

The second term in the sum does not contribute. This is expected from the derivation in reference ¹⁶, and signifies that the scattered trajectories do not contribute to the VACF because of cancellation when averaging over direction of the scattered particles. The first term can be simplified, and the limit taken,

$$S_{\mathbf{v}\mathbf{v}}(\omega) = \lim_{q \rightarrow 0} \frac{\frac{3}{2z} - \frac{1}{2z^3}}{\sqrt{\frac{m}{2kT}} q}, \quad (50)$$

$$= \frac{3kT}{m} \frac{1}{\left(s + \frac{1}{\tau_c}\right)}. \quad (51)$$

Which has an inverse Laplace transform,

$$R_{\mathbf{v}\mathbf{v}}(t) = \frac{3kT}{m} e^{-\frac{t}{\tau_c}}. \quad (52)$$

This is the expected velocity autocorrelation function for an infinite domain. This particular result could have been found by finding the single component spectrum and multiplying by the number of dimensions, for this case the information in q contained in equation (48) is removed by the average over position ($q \rightarrow 0$).

III. STOCHASTIC MOTION IN BOUNDED DOMAINS

In section II B we obtained a general expression for the propagator of our CTRWT model in an infinite domain. In this section we show how our result (33) may be used to construct the spectrum of the position and velocity auto-correlation functions in a bounded domain.

A. Spectrum of the position and velocity auto-correlation functions in a bounded domain

We consider stochastic motion within a rectangular domain of the size $\{L_x, L_y, L_z\}$. Using the method of images¹¹ each reflection from a boundary is replaced by a particle coming from an image source, the original particle being considered as leaving the physical bounded region. So the probability of arriving at a given point, $P(x, t)$ say, is given by the sum of probabilities of arriving from the original, physical source and all the image sources. As time increases more distant image sources come into play. Physically it is similar to standing between two perfect facing mirrors.

For each source point there is a set of image points, one each in a lattice of repetitions of the physical domain.

When we use this probability function to calculate averages of functions of position the probability $P(x, t)$ has to be averaged over all possible starting positions in the physical cell

and summed over all image points. This is equivalent to integrating the infinite domain probability function over all possible source points. For a more complete description refer to ^{11,15,18,19}.

The procedure can be clearly seen, for example, by considering the position coordinate as the function to be averaged. In this example as we go along the coordinate (in the positive direction) in the physical cell the coordinate increases. As we cross the boundary into the image cell the image coordinate reaches a maximum at the boundary and then decreases (negative slope). If we continue in this fashion the coordinate function will be a simple triangle wave, zero at the origin (asymmetric), with amplitude $L_x/2$, and period $2L_x$, the size of the physical cell being given by L_x .

Periodic functions can be represented in a Fourier series, for the triangle wave representing the position coordinate in the image cells centered at the origin we have,

$$\tilde{x}(x) = \sum_{n=\text{odd}} -i^n \frac{2L_x}{\pi^2 n^2} e^{i \frac{\pi n}{L_x} x}. \quad (53)$$

The spectrum of the position correlation function can thus be written in terms of the periodic varying function, \tilde{x}

$$S_{xx}(\omega) = \frac{1}{8\pi^3 L_x L_y L_z} \int_{-L/2}^{L/2} d^3 \mathbf{x}_0 \int_{-\infty}^{\infty} d^3 \mathbf{x} \int_{-\infty}^{\infty} d^3 \mathbf{q} \tilde{x} x_0 p(q, \omega) e^{-i \mathbf{q} \cdot (\mathbf{x} - \mathbf{x}_0)}, \quad (54)$$

where $p(q, \omega)$ is the conditional density found in equation (33). Integration over y and z gives $2\pi\delta(q_y)$ and $2\pi\delta(q_z)$, respectively. Due to the normalization in equation 54, subsequent integration over y_0 and z_0 will give unity. Integration over x gives $\sum_n -i^n \frac{2L_x}{\pi^2 n^2} 2\pi\delta\left(q_x - \frac{\pi n}{L_x}\right)$, due to the definition of \tilde{x} in equation (53) where the sum is over n , where n are odd integers,

$$S_{xx}(\omega) = \frac{1}{L_x} \sum_{n=\text{odd}} -i^n \frac{2L_x}{\pi^2 n^2} \int_{-L/2}^{L/2} dx_0 x_0 p\left(q = |q_x| = \frac{\pi|n|}{L_x}, \omega\right) e^{i \frac{\pi n}{L_x} x_0}. \quad (55)$$

Integration over x_0 , and taking the even extension of the causal function as above, yields,

$$S_{xx}(\omega) = \sum_{n=\text{odd}} \frac{4L_x^2}{\pi^4 n^4} p\left(|q_x| = \frac{\pi|n|}{L_x}, \omega\right). \quad (56)$$

For the velocity autocorrelation function we have,

$$S_{vv}(\omega) = \omega^2 \sum_{n=\text{odd}} \frac{4L_x^2}{\pi^4 n^4} p\left(\frac{\pi|n|}{L_x}, \omega\right). \quad (57)$$

B. Long time tails arise in diffusive motion in bounded domains.

The series expansion (56) for the spectrum of the position auto-correlation function is universal, it is valid for any mean free path from the quasi-ballistic ($\xi = \tau_c/\tau_b >> 1$) to the diffusive ($\xi << 1$) regime of motion. In this section we obtain closed-form expressions valid in the diffusive regime.

We start from equation (33),

$$p(q, \omega) = 2\text{Re} \left[\frac{\sqrt{\frac{m\pi}{2kT}} \frac{1}{q} e^{z^2} \text{erfc}(z)}{1 - \sqrt{\frac{m\pi}{2kT}} \frac{1}{q\tau_c} e^{z^2} \text{erfc}(z)} \right] = 2\text{Re} \left[\tau_c \left(\frac{1}{1 - \sqrt{\frac{m\pi}{2kT}} \frac{1}{q\tau_c} e^{z^2} \text{erfc}(z)} - 1 \right) \right], \quad (58)$$

where z is given by (31).

Assuming that the propagator is the even extension of the casual conditional probability $P(x, t)$, the spectrum of the position auto-correlation function in a finite system of size L_x reads ¹¹, (56)

$$S_{xx}(\omega) = \frac{8L_x^2}{\pi^4} \sum_{n=1,3,\dots}^{\infty} \frac{p(q_n, \omega)}{n^4}, \quad (59)$$

where,

$$z_n = \sqrt{\frac{m}{2kT}} \frac{1 + i\omega\tau_c}{q_n\tau_c}, \quad (60)$$

$$q_n = \frac{n\pi}{L_x}. \quad (61)$$

As shown in appendix A 1 the result is,

$$S_{xx}(\omega') = \frac{2\tau_c L_x^2 \xi^2}{\omega'^2 (1 + \omega'^2)} (1 - \Delta[\xi, \omega']) \quad (62)$$

where $\xi = \tau_c/\tau_b$, $\omega' = \omega\tau_c$, and

$$\Delta(\xi, \omega') = \frac{\sqrt{2}\xi}{(\omega')^{1/2}(1+\omega'^2)} \frac{\sin\left(\frac{\sqrt{\omega'}(1+\omega')}{\sqrt{2}\xi}\right)(1+2\omega'-\omega'^2) + \sinh\left(\frac{(1-\omega')\sqrt{\omega'}}{\sqrt{2}\xi}\right)(1-2\omega'-\omega'^2)}{\cos\left(\frac{\sqrt{\omega'}(1+\omega')}{\sqrt{2}\xi}\right) + \cosh\left(\frac{(-1+\omega')\sqrt{\omega'}}{\sqrt{2}\xi}\right)}. \quad (63)$$

Going back to original variables ω, τ_c, τ_b in the prefactor, noting that $\left(\frac{L_x}{\tau_b}\right)^2 = kT/m$ and using $D = \frac{kT}{m}\tau_c$, (D is the diffusion coefficient), we find,

$$S_{xx}(\omega) = \frac{2D}{\omega^2(1+(\omega\tau_c)^2)} (1 - \Delta(\xi, \omega\tau_c)). \quad (64)$$

Note, that our result (63,64) for the spectrum of the position correlation function is valid for any ω from 0 to ∞ as long as $\tau_c \ll \tau_b$, which is the condition for diffusive motion. Taking the limit $\omega \rightarrow 0$ we obtain,

$$S_{xx}(0) = \frac{L_x^4}{60D} - \frac{1}{6}L_x^2\tau_c = \frac{L_x^4}{60D} (1 - 10\xi^2). \quad (65)$$

which is valid for the “non-adiabatic” regime of motion $\omega \ll 1/\tau_d$. Here, the first term is well known from “classical” diffusion theory,⁶. The second term, $\sim 10\xi^2$ is the next order correction from our CTRWT model. When diffusion theory is valid the correction is very small.

We see that the prefactor in (64) does not involve any information on the system size, while the term $\Delta(\xi, \omega\tau_c)$ depends on the size of the system. Thus the prefactor represents the spectrum for an infinite system $S_{xx}^{\text{inf}}(\omega)$ while the term $\Delta(\xi, \omega\tau_c)$ is a correction due to the finite size,

$$S_{xx}(\omega) = S_{xx}^{\text{inf}}(\omega) [1 - \Delta(\xi, \omega\tau_c)], \quad (66)$$

$$S_{xx}^{\text{inf}}(\omega) = \frac{2D}{\omega^2(1+\omega^2\tau_c^2)}. \quad (67)$$

We may greatly simplify (63) noting that for large values of the argument $\frac{\sqrt{\omega\tau_c}(1-\omega\tau_c)}{\sqrt{2\xi}} \gg 1$ the hyperbolic functions dominate and (63) reduces to:

$$\Delta(\xi, \omega\tau_c) \approx \text{sign}(1 - \omega\tau_c) \frac{\sqrt{2}\xi (1 - 2\omega\tau_c - \omega^2\tau_c^2)}{(\omega\tau_c)^{1/2} (1 + \omega^2\tau_c^2)}. \quad (68)$$

We illustrate the frequency dependence of the finite size corrections (63), solid line, and (68), dashed line, on Figure 1.

For $\omega\tau_c \ll 1$, the condition $\frac{\sqrt{\omega\tau_c}(1-\omega\tau_c)}{\sqrt{2\xi}} \gg 1$ reduces to $\omega\tau_c \gg 2\xi^2$, or $\omega\tau_d \gg 2\pi^2$. This condition together with $\omega\tau_c \ll 1$ constitutes the “classical” conditions for the “adiabatic” regime of spin-motion: $1/\tau_d \ll \omega \ll 1/\tau_c$. When these conditions are fulfilled,

$$\Delta(\xi, \omega\tau_c) \approx \frac{\sqrt{2}\xi}{(\omega\tau_c)^{1/2}}. \quad (69)$$

From analysis of Figure 1 we conclude that the expression (68) indeed gives an excellent approximation to the exact result (63) for the “adiabatic” and “super-adiabatic” regimes of spin-motion. Figure 2 shows the normalized position correlation spectrum $S_{xx'}(\omega)/(D\tau_c^2)$ calculated from (63, 64) as well as using approximation (68).

1. Spectrum of the correlation function of a single velocity component and long time memory in finite systems.

In this section we show the existence of a long time tail in the velocity autocorrelation function that arises only in the bounded domain. In free space it was shown in equation (52) that there is no long time tail, and the velocity autocorrelation decays exponentially in time.

The spectrum of the correlation function of a single velocity component $S_{v_x v_x}(\omega)$ may be found from,

$$S_{v_x v_x}(\omega) = \omega^2 S_{xx}(\omega), \quad (70)$$

which gives,

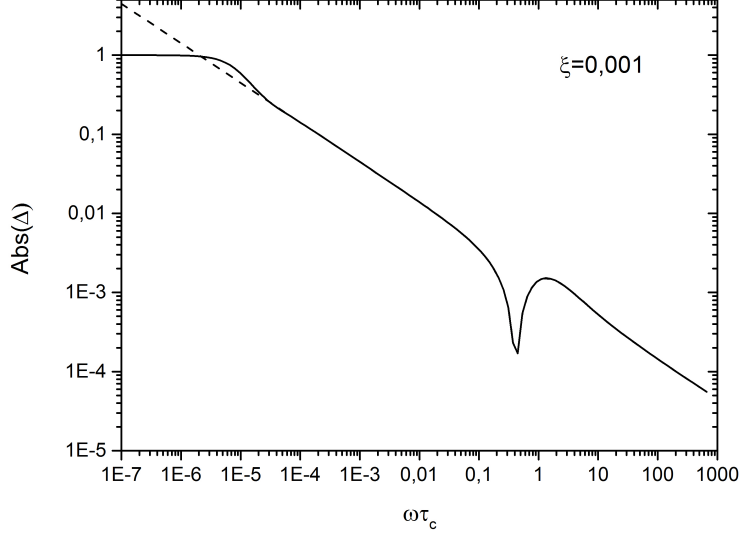


FIG. 1. Correction to the spectrum of position correlation function (63) due to the finite size of the system, (solid line). Approximate correction (68), (dashed line). For $\omega\tau_c \ll 1$ the correction is negative, it has irregularities in the vicinity of $\omega\tau_c \sim 1$, where both functions abruptly change sign when $\omega\tau_c = 1$. However, the detailed behavior of the correction for $\omega\tau_c \gtrsim 1$ is of minor importance since its relative magnitude is small.

$$S_{v_x v_x}(\omega) = S_{v_x v_x}^{\text{inf}}(\omega)(1 - \Delta(\xi, \omega\tau_c)), \quad (71)$$

$$S_{v_x v_x}^{\text{inf}}(\omega) \approx \frac{2D}{(1 + \omega^2 \tau_c^2)}, \quad (72)$$

where the finite size correction, $\Delta(\xi, \omega\tau_c)$, is the same as for the spectrum of the position correlation function.

Figure 3 shows the exact spectrum of the correlation function of a single velocity component given by (63, 71, 72), solid line, as well as the spectrum obtained using the approx-

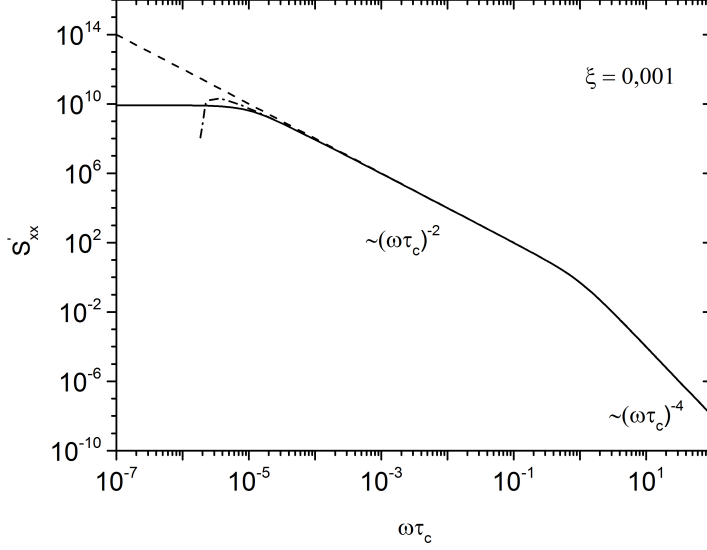


FIG. 2. Normalized position correlation spectrum $S_{xx}(\omega)/(2D\tau_c^2)$ calculated from (64), using the exact finite size correction (63) (solid line), using the approximate correction (68), (dashed line), and for the infinite system (67), (dot-dashed line). Saturation of the spectrum for $\omega\tau_d < 1$ is a signature of the finite size.

imation (68), dashed line, and the spectrum for an infinite domain (72), dot-dashed line.

Applying the inverse Fourier transform to (72) we recover the well known result for the velocity correlation function for an infinite domain (52):

$$R_{v_x v_x}^{\text{inf}}(t) = \frac{kT}{m} e^{-|t|/\tau_c}. \quad (73)$$

The inverse Fourier transform for the exact result (63, 71, 72) is unknown. However, the relatively simple form of (68) allows an inverse Fourier transformation. For $\tau_d \gg t \gg \tau_c$ we obtain,

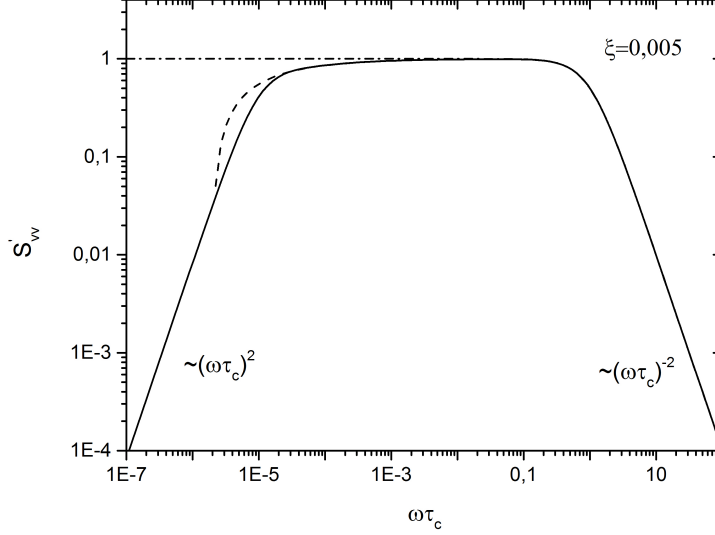


FIG. 3. Normalized spectrum of the correlation function for a single velocity component $S_{v_x v_x}/D$ calculated according to (71), using the exact finite size correction (63) (solid line), using the approximate correction (68) (dashed line), and for the infinite system (72), (dot-dashed line). The low frequency cut-off for $\omega\tau_c \ll \xi^2$ is a signature of finite size systems.

$$R_{v_x v_x}(t) \approx R_{v_x v_x}^{\text{inf}}(t) - \frac{2}{\sqrt{\pi}} \xi \frac{kT}{m} \left(\frac{t}{\tau_c} \right)^{-1/2}. \quad (74)$$

One can see that the finite size correction has the form of a long-time tail $\sim (t/\tau_c)^{-1/2}$ with a relative magnitude of the order of $\xi = \tau_c/\tau_b$.

Both solutions (73, 74) are illustrated in figure 4.

For very short times, $t \ll \tau_c$, all the results decay exponentially with a time constant τ_c . For longer times only $R_{v_x v_x}^{\text{inf}}(t)$ decays exponentially. The velocity correlation function $R_{v_x v_x}(t)$ for a finite system has a very different behavior: for longer times it crosses the τ/τ_c axis from positive values to negative ones (at the position where a spike is observed on the log-log plot), and for even later times it goes back toward the τ/τ_c axis being negative.

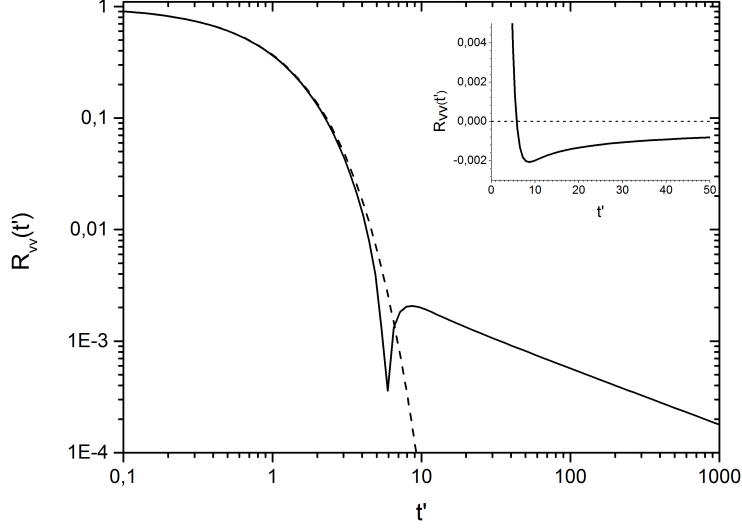


FIG. 4. Normalized velocity correlation function $R'_{vv}(t') = \frac{m}{kT} R_{vv}(t')$, where $t' = \frac{t}{\tau_c}$. From the analytic result (74) valid for $t \ll \tau_d$, solid line. For the infinite system (73), dashed line. Negative spikes correspond to positions where functions change their sign. The insert shows the same function but in linear scale.

It stays negative for very long times, until τ approaches τ_d , slowly decaying in magnitude according to a power law $\sim t^{-1/2}$. It may be shown, see appendix (A 1), that for even longer times, $\tau \gg \tau_d$, it again decays exponentially with time constant τ_d . This negative long time tail, $\sim t^{-1/2}$, in the velocity correlation function is the same for 1 D, 2 D, and 3 D systems and arises due to reflections from the system boundaries. This is in agreement with the 1 dimensional treatment examined in reference¹⁵. This is in contrast to molecular dynamics where long range hydro-dynamic forces continuously act on the trajectories. These forces tend to produce cross correlation between motion in different directions, for example vorticular motion. The cross-correlation is examined in reference²⁰. See also²¹. Including cross-correlation of such kind leads to "long time tails" $\propto t^{-d/2}$, where d represents the

number of dimensions in the system. However, in systems of a relative low density gas, the cross correlations resulting from hydro-dynamic forces are suppressed, and our result completely describes the dynamics.

We can see the reason for the difference between our result and previous results showing a tail ($\sim t^{-d/2}$) by examining reference²⁰. Equation (1) in that paper, while calculating the correlation function of a single velocity component, is a function of $k'^2 = \sum_{i=1}^d k_i'^2$. However in calculating the position correlation function $\langle x_i(0) x_i(\tau) \rangle$ for each i , the dependence on the other components, $j \neq i$, integrates out due to normalization of the conditional probability so the correlation $\langle x_i(0) x_i(\tau) \rangle$ only depends on k_i . Using (A11) to get the correlation function of the individual velocity components v_i we see that these each depend only on its particular k_i . The total velocity autocorrelation function $\langle \mathbf{v}(t) \cdot \mathbf{v}(t - \tau) \rangle$ is then the sum of d such terms. The result is then a sum of terms ($\sim t^{-1/2}$). Equation (1) in²⁰ contains products of functions of the different k_i' s and this results in the ($\sim t^{-d/2}$) behavior as shown in equations (4), (16) and (18) of that work and implies correlations between the different directions of motion which do not occur in diffusion theory.

Another aspect of the long-time tail is a non-linear behavior of the mean square displacement,

$$\langle x^2(t) \rangle = 2 \int_0^t (t - \tau) \langle v_x(0) v_x(\tau) \rangle d\tau = 2 \frac{kT}{m} \int_0^t \left(e^{-t/\tau_c} - \frac{2}{\sqrt{\pi}} \xi \left(\frac{t}{\tau_c} \right)^{-1/2} \right) (t - \tau) d\tau, \quad (75)$$

$$\approx 2Dt \left(1 - \frac{8}{3\sqrt{\pi}} \sqrt{\frac{t}{\tau_d}} \right). \quad (76)$$

Recall that our results (74) and, hence, (76) are valid for $\tau_c \ll t \ll \tau_d$. Again, we see that for not too long times $t \gg \tau_c$ the diffusion is a stationary Markovian process with,

$$\langle x^2(t) \rangle = 2Dt, \quad (77)$$

while for longer times, but still $t \ll \tau_d$, reflections from the boundaries will alter the

linear dependence (77). While our correction is small it is an indication of how the diffusion process eventually ends for $t \gg \tau_d$ in a homogeneous steady state with,

$$\langle x^2 (t \gg \tau_d) \rangle = \langle x^2 \rangle. \quad (78)$$

As our results for the propagator have been shown to agree with diffusion theory in the limit $\xi = \frac{\tau_c}{\tau_b} \ll 1$, we expect that the long time tail will also occur in the classical diffusion theory. We show this in an appendix.

C. Spectrum of the bounded domain position correlation function in the ballistic or diffusive limits.

1. Diffusive Region

In the diffusion limit, the spectrum of the position autocorrelation function is observed to stratify into three regimes shown in figure 2.

a: the non adiabatic regime, defined by $\omega \ll \tau_d^{-1}$, with spectrum,

$$S_{xx}(\omega) \approx S_{xx}(0) \approx \frac{1}{60} \frac{L_x^4}{D}. \quad (79)$$

b: the adiabatic regime, defined by $\tau_d^{-1} \ll \omega \ll \tau_c^{-1}$, with spectrum,

$$S_{xx}(\omega) \approx \frac{2D}{\omega^2}. \quad (80)$$

c: the super-adiabatic regime, defined by $\tau_c^{-1} \ll \omega$, with spectrum,

$$S_{xx}(\omega) \approx \frac{2D}{\omega^4 \tau_c^2}. \quad (81)$$

Where the diffusion coefficient, $D = \frac{k_B T}{m} \tau_c$, and the diffusion time, $\tau_d = \frac{L^2}{\pi^2 D}$, the time constant for the lowest diffusion mode.

2. *Quasi-Ballistic motion*

In this section we will discuss some general properties of the spectrum of the position-position auto-correlation function (56) in the case of quasi-ballistic motion.

With decreasing pressure, the diffusion time decreases and the collision time, τ_c , increases. The motion is no longer diffusive when the time to cross the restricted volume approaches the collision time, $\tau_b = \frac{L}{\sqrt{\frac{k_b T}{m}}} \lesssim \tau_c$. This is considered to be the quasi-ballistic region, and in this region there exists no adiabatic regime, where $S_{xx}(\omega) \propto \omega^{-2}$, only two distinct regions are found.

Considering the limit $\xi = \tau_c/\tau_b \gg 1$ with the spectrum given by equation (56) leads us to distinguish three different regimes:

a: The non adiabatic regime or low frequency region, $\omega \ll 1/\tau_c \ll 1/\tau_b$ and $|z_n| \ll 1$. In this regime we can replace $\exp(z_n^2) \operatorname{erfc}(z_n)$ in equations (30, 33) by equation (34),

$$p(q_n, \omega) \approx 2 \left(\frac{1}{1 - \frac{1}{\sqrt{2\pi n \xi}}} - 1 \right) \approx \frac{2\tau_c}{n\sqrt{2\pi\xi}},$$

with the spectrum of the position auto-correlation function given by equation (56),

$$S_{xx}(\omega) \approx \frac{16L_x^2}{\pi^4} \frac{1}{\sqrt{2\pi\xi}} \tau_c \sum_{n=1,3,\dots}^{\infty} \frac{1}{n^5} = \frac{31L_x^2 \tau_b \zeta(5)}{2\sqrt{2\pi} \frac{9}{2}}, \quad (82)$$

where $\zeta(n)$ is the Riemann zeta function.

b: The intermediate regime defined by $1/\tau_c \ll \omega \ll \sqrt{2\pi}/\tau_b$. In this regime z_n is mostly imaginary but still $|z_n| \ll 1$ and the low z expansion is valid leading to the same spectrum as above.

c: the super-adiabatic regime or high frequency region, defined by $\sqrt{2\pi}/\tau_b \ll \omega$, with spectrum found according to the large $|z| \gg 1$ expansion, equation (34), of the conditional density, equation (33),

$$S_{xx}(\omega) \approx \frac{2D}{\omega^2 (1 + (\omega\tau_c)^2)} \approx \frac{2D}{\omega^4 \tau_c^2},$$

$$S_{v_x v_x}(\omega) \approx \frac{2D}{(\omega\tau_c)^2}.$$

Figure 5 shows spectra of the position correlation function for different regimes of motion from diffusive to quasi - ballistic, it is observed that scaling $\xi = \tau_c/\tau_b$ shifts the transition frequency for the quasi-ballistic non-adiabatic to super-adiabatic regimes, when $\xi < 1$ the diffusion region is observed. It is interesting to compare the result for the spectrum of the position correlation function given by our CTRWT model, equations (33,56), with the prediction¹¹ for the CTRW in a “frozen environment”.

Fig. 5 shows the evolution of the spectrum of position auto-correlation function from the diffusive ($\xi = .02$) to the quasi-ballistic ($\xi = 50$) regime of motion. Solid lines represent the predictions of our thermalizing CTRWT model, dotted lines corresponds to the model of CTRW in the “frozen environment”¹¹.

For quasi - ballistic motion in the “frozen environment” model collisions with the boundaries lead to the formation of resonances, (for details see¹¹). In this model the character of the structure of the resonances, as well as their width, depends on the parameter ξ and the number of dimensions in the system. The higher is ξ the more narrow are the resonances. For the diffusive regime of motion ($\xi \ll 1$) the resonance structure is fully washed out and the prediction of all three models: our model of CTRWT, CTRW in “frozen environment” and classical diffusion theory⁶ are indistinguishable.

The resonances in the ballistic region would be smoothed out by averaging the ‘frozen scatterer’ spectrum over a Maxwell-Boltzmann velocity distribution, however in the zero frequency limit the velocity average of the spectrum diverges. Furthermore velocity averaging the single velocity spectrum in the diffusion region gives results which depend on the number of dimensions as shown in figure 6, in disagreement with the thermalization model presented here.

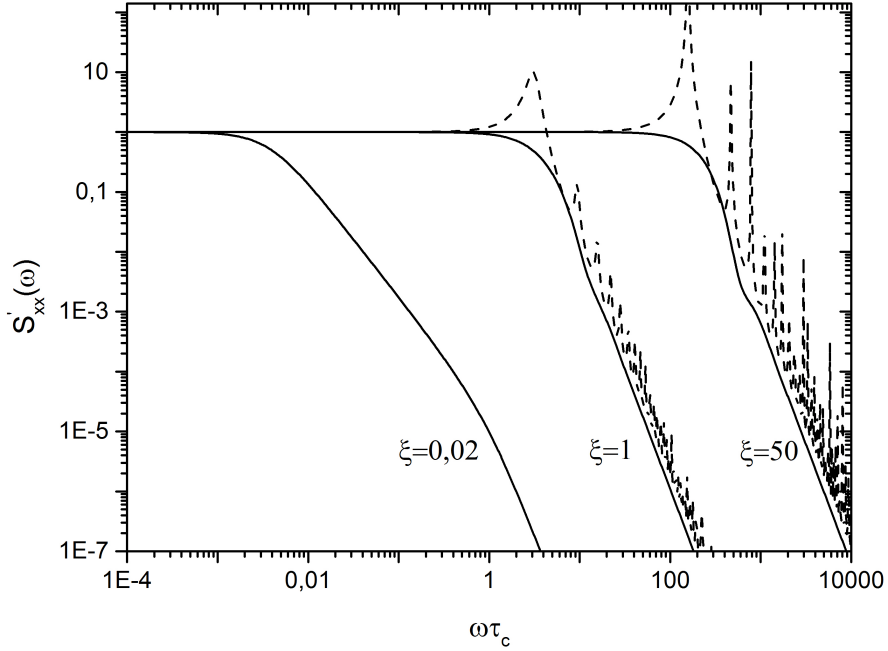


FIG. 5. The normalized spectrum of the position autocorrelation function $S'_{xx}(\omega) = \frac{S_{xx}(\omega)}{S_{xx}(0)}$, a comparison of the frozen picture with the thermalization picture in different regimes, diffusive ($\xi = 0.02$), intermediate ($\xi = 1$), and quasi-ballistic ($\xi = 50$). Solid lines represent predictions of our CTRWT model, dotted lines correspond to the CTRW in the "frozen environment". For diffusive motion ($\xi = 0.02$) all models: CTRWT, CTRW in the "frozen environment", and classical diffusion theory give predictions which are indistinguishable in this plot.

D. Application of the bounded domain correlation functions

Another correlation function of particular physical interest is the position-velocity correlation function as it determines the frequency shift linear in the electric field of spins precessing in magnetic and electric fields. This is important in the search for electric dipole moments (edm), where the presence of an edm results in frequency shifts which are also linear in

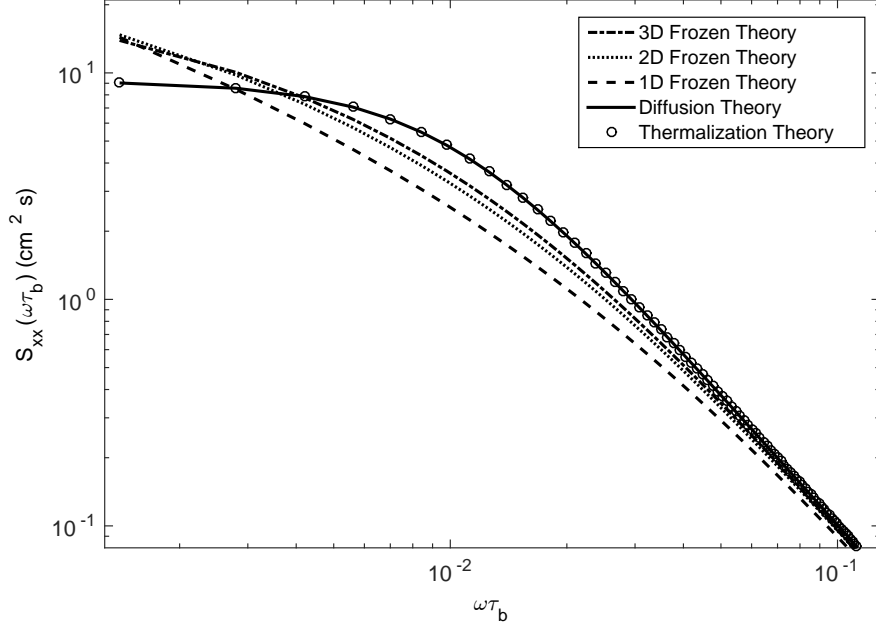


FIG. 6. The thermalization model compared to the "frozen" CTRW models, and diffusion theory for $T=300$ mK, in the diffusion limit, $\omega\tau_c \ll 1$. Diffusion theory is accurate in this regime. We use the diffusion coefficient given by reference²². It is seen that the "frozen" CTRW models diverge from diffusion theory at low frequencies.

the applied electric field^{7,8}. With the use of integration by parts, the frequency shift can be written in terms of the imaginary component of the Fourier transform of the position auto-correlation function,^{3,23,24}

$$\begin{aligned} \delta\omega = & -\omega \frac{\gamma^2 E}{c} \text{Im} \left[\int_0^\infty e^{-i\omega\tau} \langle B_x(t)x(t+\tau) + B_y(t)y(t+\tau) \rangle d\tau \right] \\ & - \gamma^2 \frac{E}{c} \langle B_x x + B_y y \rangle, \end{aligned} \quad (83)$$

here E is the strength of the electric field applied in the z direction, and $B_{x,y}$ represents a perturbing magnetic field. $\langle \cdot \rangle$ represents an ensemble average. The frequency ω is determined

by the applied holding field B_0 , also in the z direction,

$$\omega = \gamma B_0. \quad (84)$$

The field B_x in equation (83) is a perturbation on the holding field B_0 manifest from the inevitable inhomogeneities of laboratory magnets. For accurate predictions of the relaxation and frequency shifts accounting for linear and quadratic terms are enough ²⁵, any higher order terms are negligible. Due to the correlation between field and position only asymmetric terms contribute, therefore only contributions from linear inhomogeneities are required for an accurate prediction. Therefore, we take,

$$B_{x,y} \propto x, y,$$

and the phase shift due to the x component is proportional to the spectrum of the position autocorrelation function,

$$\delta\omega \propto \omega \text{Im} [S_{xx}(\omega)] + \langle xx \rangle. \quad (85)$$

In this case $S_{xx}(\omega)$ is the spectrum obtained by using $p(q, s = i\omega)$, where $p(q, s)$ is the causal conditional density. A similar expression exists for the y component.

The thermalization model of the random walk presented in this work is now used to predict the phase shift of ^3He , Larmor precessing in a dilute solution in superfluid ^4He ,²⁶.

For a number density ratio $^3\text{He}:^4\text{He} < 10^{-7}$, ^3He - ^3He collisions can be ignored and collisions with the excitations in the superfluid dominate. The system is taken to be a rectangle of 10.2 by 40 by 7.6 cm. In superfluid helium viscosity is absent ²⁷ and the ^3He behaves as if it were in a vacuum with an increased mass $m_{^3\text{He}}^* = 2.4m_{^3\text{He}}$. The ^3He will thermalize by scattering on the excitations, phonons and rotons, in the superfluid. When the temperature of the superfluid is brought below 500 mK, phonons become the dominant excitation. In such a system the diffusion coefficient was measured ^{28,29} and the data was fit well by the equation,

$$D = \frac{1.6}{T^7}. \quad (86)$$

We convert this to a collision time according to equation (37),

$$\tau_c = 1.6 \frac{m}{kT^8}.$$

The predicted result is shown in figure 7 and as a function of temperature in figure 8 along with the result from³⁰. The treatment of temperature is different in reference³⁰, where the single velocity random walk result is averaged over a Maxwellian distribution of velocities. However an important prediction remains; a strong dependence on temperature of the magnitude of the linear in E shift. Therefore varying the temperature is a tool to mitigate and study the effect.

1. Comparison of the CTRWT model with Monte-Carlo simulations

A comparison with 1D 2D and 3D Monte Carlo simulations are done on 10^3 trajectories for 2×10^6 time steps. The trajectories are specific to ^3He at very low concentrations in superfluid ^4He at 400 mK, described in the previous section III D. In this regime the mean free path is determined by collisions with phonons in the superfluid. Upon a collision the new velocity was determined according to the isotropic 3D Maxwellian distribution. The trajectories are confined by specular wall collisions inside a rectangular volume 10.2 by 7.6 by 40 cm. The theoretical spectrum of the position autocorrelation function (56) is shown in figure 9, and compared to the results of the simulations. Figure 10 shows the position autocorrelation function, a function of time. The theoretical value of the position autocorrelation function is found from numerical inversion of the theoretical result for the spectrum except at $t = 0$. Due to the finite nature of the numerical inversion the $t = 0$ point is obtained by the mean squared average of position, $\langle x(t)x(t) \rangle$.

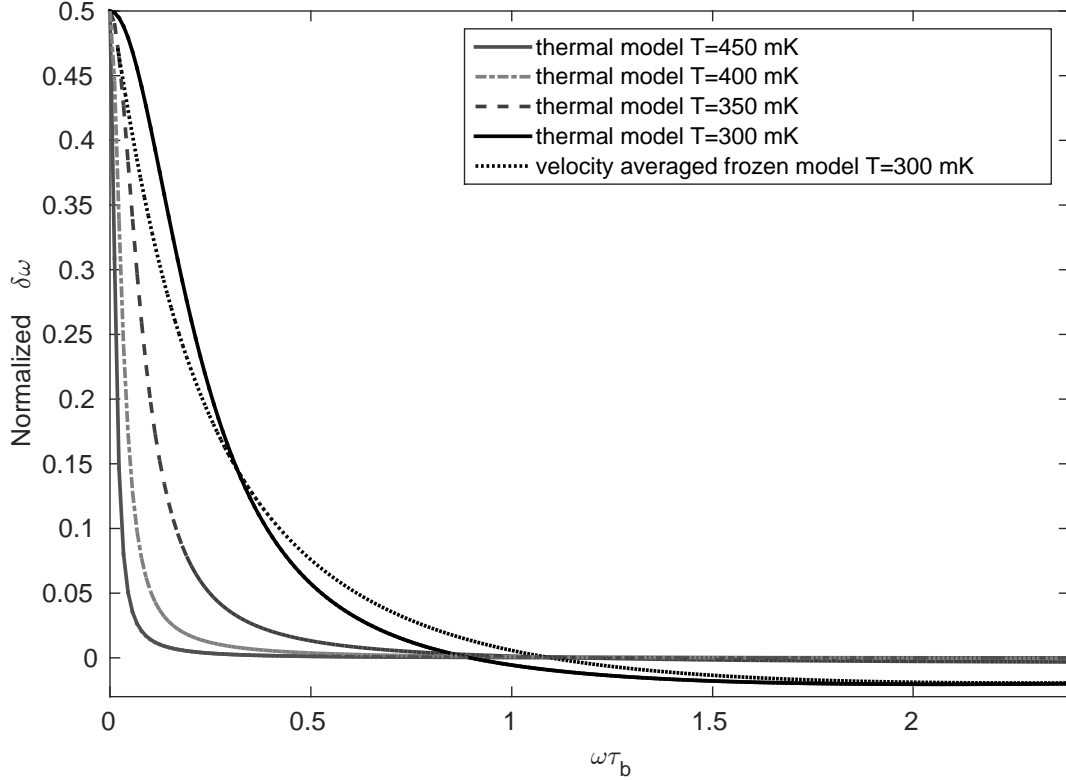


FIG. 7. The normalized spectrum of the linear in E phase shift bounded to a length of 40 cm for dilute ^3He dissolved in superfluid ^4He , with temperature as a parameter. All the solid curves are derived from the thermalization model, the dashed line is the velocity averaged frozen model³⁰.

IV. CONCLUSION

We have constructed a microscopic theory of the propagator (conditional probability density) for a persistent random walk where the particles undergo either Markovian stochastic scattering events or $1/v$ scattering satisfying detailed balance and maintaining thermal equilibrium in both cases. For a gas with a Maxwell-Boltzmann velocity distribution we obtain a relatively simple expression for the propagator. The result is independent of the number of dimensions considered, contrary to the "frozen" walk (a CTRW with fixed velocity) where the number of dimensions in the walk strongly effect the resonant structure of the corre-

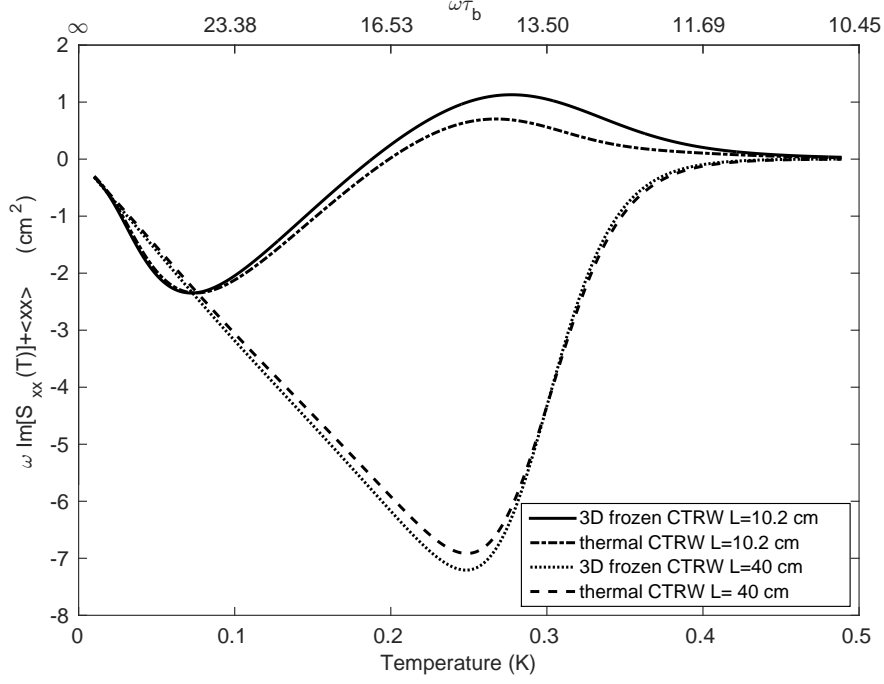


FIG. 8. The relative phase shift predicted from the thermalization model is compared to the single velocity models averaged over velocity. As the temperature decreases, and $\omega\tau_b$ ($L = 40$ cm) increases, the models diverge.

lation functions generated by the walk¹¹, and valid for all values of the scattering mean free path from the quasi-ballistic to the diffusion regime of motion. We have shown directly that our results go over into the standard diffusion theory for short collision times (short mean free paths). We have shown how the results can be applied to bounded regions using the method of images and have given results for the position-position, position-velocity and velocity-velocity correlation functions, all of which have direct applications in calculating frequency shifts and relaxation rates in nmr systems. One application is to the calculation of the NMR phase shift of ^3He in superfluid ^4He in a magnetic and electric field. The results differ somewhat from the previous results obtained by averaging the 'frozen' walk results over a Maxwell velocity distribution.

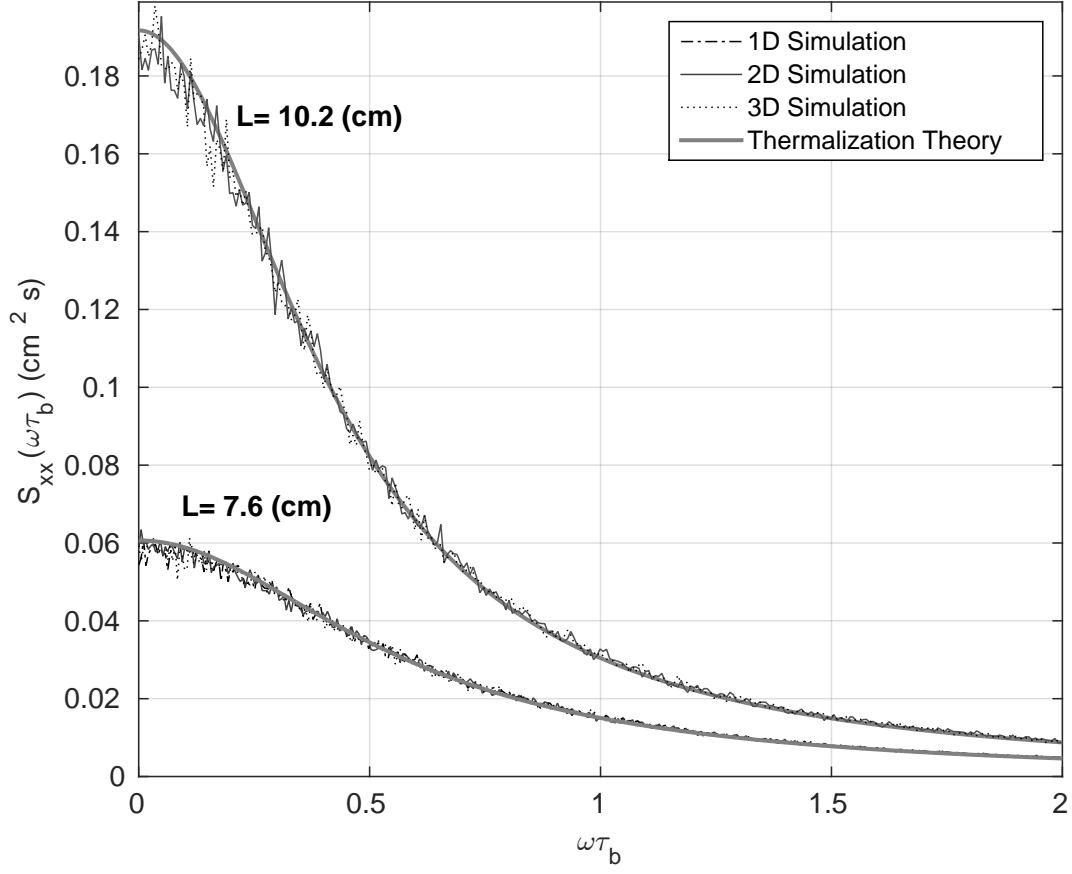


FIG. 9. The spectrum of the position autocorrelation function, a comparison of theory to 1D, 2D and 3D simulations with thermalizing collisions for a temperature corresponding to 400 mK in the bulk. Good agreement is observed. Plotted are the correlation functions for one direction in which the cell length is either 7.6 cm or 10.2 cm. The third dimension in the 3D simulation is 40 cm, it is not shown.

The method can be applied to inhomogeneous fields of any shape. We have discovered a universal long-time tail $\propto t^{-1/2}$ independent of dimensionality in bound systems. We emphasize that this long-time tail is expected only for bounded systems and it is diminished with the increase of the system size. While we show that this effect is predicted by the standard diffusion theory in agreement with¹⁵ who found a similar long-time tail by solving

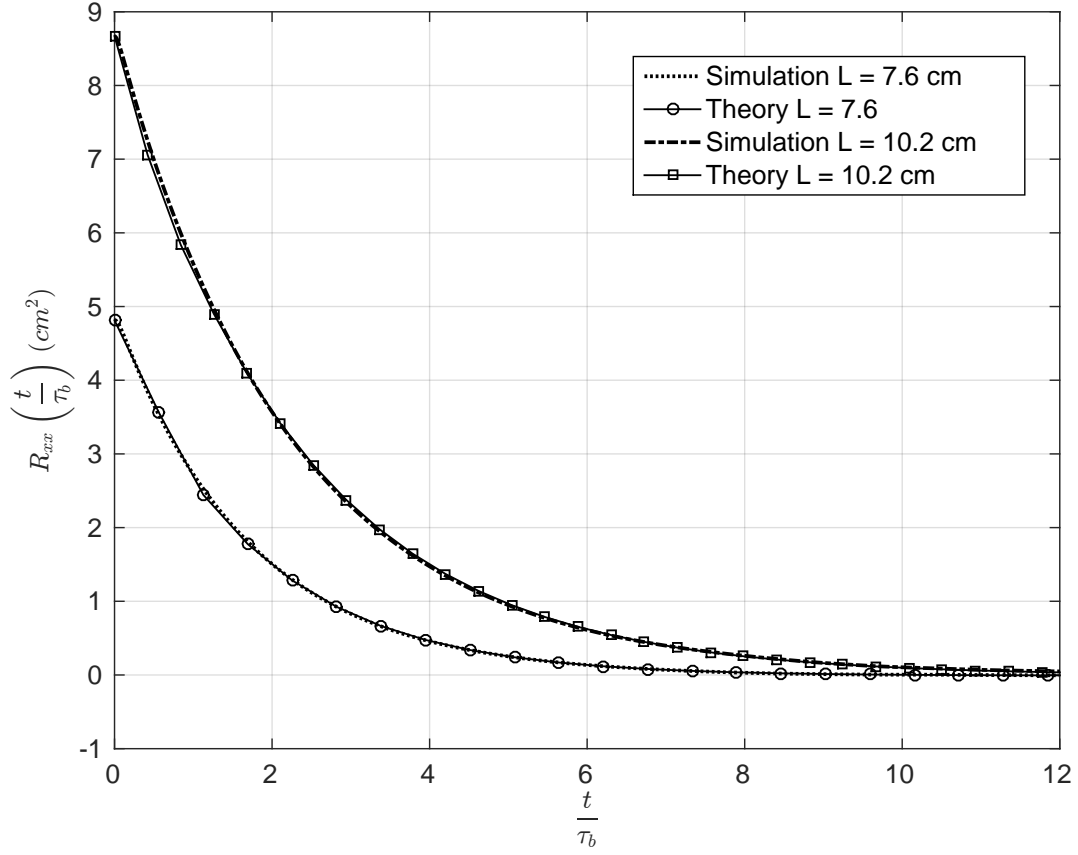


FIG. 10. The position autocorrelation function. The 3D Simulation is compared to thermalization theory. Good agreement is observed.

the one dimensional Langevin equation, the independence of dimensionality does not seem to have been noticed before.

V. ACKNOWLEDGMENTS

We are grateful for fruitful discussion with Efim Katz on the long-time tail problem and with Bart McGuyer concerning scattering kernels. We are grateful for the referee calling our attention to the external force problem in reference¹³. This work was supported in part by

the US Department of Energy under Grant No. DE-FG02-97ER41042 and the US National Science Foundation under Grant No. 1506459.

Appendix A: Appendix

1. Calculation of the long-time tail from the thermalization model

It is useful to introduce dimension-less variables,

$$\xi = \frac{\tau_c}{\tau_b} \text{ and } \omega' = \omega\tau_c. \quad (\text{A1})$$

In terms of new variables equations (58, 59) yield

$$z_n = \frac{1 + i\omega'}{\sqrt{2\xi\pi n}}, \quad (\text{A2})$$

$$S_{xx}(\omega') = \frac{16\tau_c L_x^2}{\pi^4} \left(-\frac{\pi^4}{96} + \sum_{n=1,3,\dots}^{\infty} \frac{1}{n^4} \text{Re} \left[1 \middle/ \left(1 - \left(\sqrt{2\pi n \xi} \right)^{-1} e^{z_n^2} \text{erfc}(z_n) \right) \right] \right). \quad (\text{A3})$$

The diffusive regime of motion is defined by $\xi \ll 1$, thus for not too high n , $z_n \gg 1$. Due to the strong cut-off by the prefactor n^{-4} in (A3) only a few lower order terms are effective, which allows us to apply the asymptotic expansion for $\text{erfc}(z)$ valid for $z \gg 1$,³¹ 7.1.23,

$$e^{z^2} \text{erfc}(z) \approx \frac{1}{\sqrt{\pi}z} \left(1 - \frac{1}{2z^2} \right). \quad (\text{A4})$$

Using (A4) we can write for the sum in (A3):

$$\sum_{n=1,3,\dots}^{\infty} \frac{1}{n^4} \text{Re} \left[1 \middle/ \left(1 - \frac{1}{\sqrt{2\pi n \xi}} \frac{1}{\sqrt{\pi} z_n} \left(1 - \frac{1}{2z_n^2} \right) \right) \right] \quad (\text{A5})$$

$$= \text{Re} \left[\sum_{n=1,3,\dots}^{\infty} \frac{1}{n^4} \frac{(-i + \omega')^3}{in^2\pi^2\xi^2 + \omega'(-i + \omega')^2} \right] = \text{Re} \left[\sum_{n=1,3,\dots}^{\infty} \frac{1}{n^4} \frac{(-i + \omega')/\omega'}{1 + \alpha^2 n^2} \right], \quad (\text{A6})$$

where,

$$\alpha^2 = \frac{i\pi^2\xi^2}{\omega'(-i+\omega')^2}. \quad (\text{A7})$$

The sum in (A6) converges,

$$S_n(\omega') = \sum_{n=1,3,\dots}^{\infty} \frac{1}{n^4} \frac{(-i+\omega')/\omega'}{1-\alpha^2 n^2} = \frac{(-i+\omega')/\omega'}{96} \pi \left(\pi^3 - 12\pi\alpha^2 + 24\alpha^3 \tanh\left(\frac{\pi}{2\alpha}\right) \right). \quad (\text{A8})$$

replacing α by (A7),

$$\text{Re}[S_n(\omega')] = \frac{\pi^4}{96} + \frac{\pi^4\xi^2}{8\omega'^2(1+\omega'^2)} - \text{Re} \left[\frac{(-1)^{3/4}\pi^4\xi^3 \tanh\left(\frac{(-1)^{3/4}\sqrt{\omega'}(-i+\omega')}{2\xi}\right)}{4(\omega')^{5/2}(-i+\omega')^2} \right]. \quad (\text{A9})$$

Expanding and taking the real part in (A9) we arrive at,

$$\text{Re}[S_n(\omega')] = \frac{\pi^4}{96} + \frac{\pi^4\xi^2}{8(\omega')^2(1+\omega'^2)} (1 - \Delta[\xi, \omega']). \quad (\text{A10})$$

with $\Delta[\xi, \omega']$ given by (63).

2. Calculation of the long time tail in ordinary diffusion theory

We start from the well known relation,

$$R_{v_x v_x}(t) = -\partial_t^2 R_{xx}(t). \quad (\text{A11})$$

For a 3D diffusive motion in a rectangular domain the auto-correlation function of the displacement in each direction is given by a term of the form,

$$R_{xx}(t) = \frac{8L_x^2}{\pi^4} \sum_{n=0}^{\infty} \frac{1}{(2n+1)^4} e^{-\frac{(2n+1)^2 t}{\tau_d}}. \quad (\text{A12})$$

Where,

$$\tau_d = \frac{L_x^2}{\pi^2 D}, \quad (\text{A13})$$

is the time constant for the lowest diffusion mode. Expression (A12) is valid for not too short times, $t \gg \tau_c$, (τ_c is the mean time between particle collisions). Inserting (A12) into (A11) we find, in agreement with (62) in reference¹⁵,

$$R_{v_x v_x}(t) = -\frac{8L_x^2}{\pi^4} \frac{1}{\tau_d^2} \sum_{n=0}^{\infty} e^{-\frac{(2n+1)^2 t}{\tau_d}} = -\frac{4L_x^2}{\pi^4} \frac{1}{\tau_d^2} \vartheta_2 \left(0, e^{-\frac{4t}{\tau_d}} \right), \quad (\text{A14})$$

where $\vartheta_2(u, z)$ is Jacobi theta function.

To investigate the short-time, ($t \ll \tau_d$), behavior of the Jacobi theta function we expand it in a series and keep only lowest order terms,

$$\vartheta_2 \left(0, e^{-\frac{4t}{\tau_d}} \right) \approx \frac{\sqrt{\pi} \sqrt{\tau_d}}{2\sqrt{t}}. \quad (\text{A15})$$

Inserting (A15) into (A14) we find,

$$R_{v_x v_x}(t) = -\frac{4L^2}{\pi^4} \frac{1}{\tau_d^2} \frac{\sqrt{\pi} \sqrt{\tau_d}}{2\sqrt{t}} = -\frac{2}{\pi^{1/2}} \xi \frac{kT}{m} \left(\frac{t}{\tau_c} \right)^{-1/2}. \quad (\text{A16})$$

For a longer times, ($t \gg \tau_d$), $e^{-\frac{4t}{\tau_d}} \rightarrow 0$ and we may expand $\vartheta_2(0, z)$ for $z \rightarrow 0$. Again keeping only lowest order terms,

$$R_{v_x v_x}(t) = -\frac{8L^2}{\pi^4} \frac{1}{\tau_d^2} \exp \left[-\frac{t}{\tau_d} \right]. \quad (\text{A17})$$

We see that (A16) is exactly the same as second term in (74). Hence, both Diffusion theory and our CTRWT model predicts the existence of a long-time tail (A16) in the correlation function for each velocity component. This negative tail exists for $\tau_c \ll t \ll \tau_d$, for even longer times the velocity correlation function decays exponentially with time constant τ_d , see (A17).

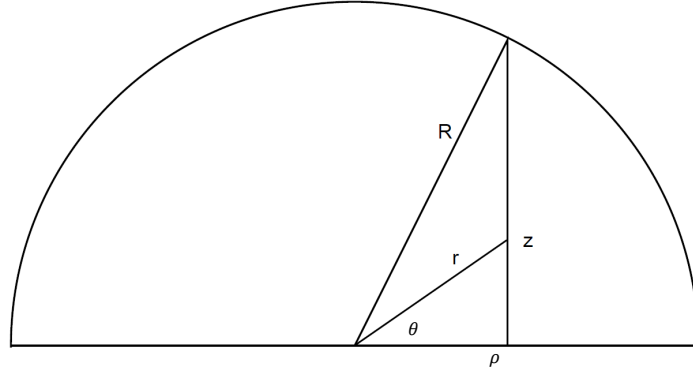


FIG. 11. Visualization of the projection from a higher dimension onto a lower dimension.

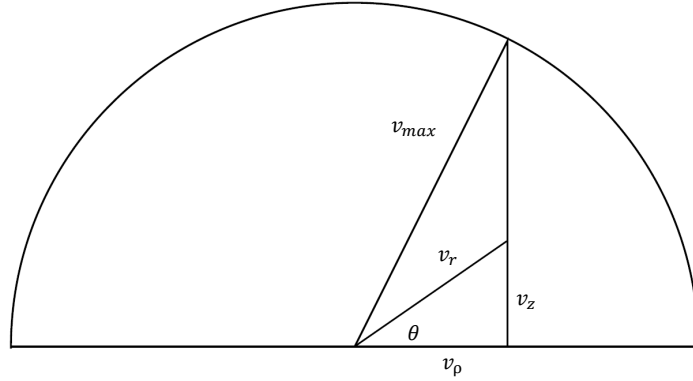


FIG. 12. Visualization of the projection from a higher dimension onto a lower dimension.

Appendix B: Cartesian Projection from 3D, equivalence for arbitrary velocity distributions.

The CTRW probability density defines how trajectories propagate and is typically used to calculate averages and correlation functions. In the case that the CTRW probability density function is isotropic, and the velocity distribution associated with the CTRW is isotropic,

and the function that is being averaged or correlated does not depend on one or more of the Cartesian coordinates, then the variable can be integrated away. The resulting function will only depend on one or two of the Cartesian coordinates. This is because cross-correlation between the different coordinates in a Cartesian system is absent. The CTRWT can be expressed in terms of the spectrum of the $F(\mathbf{r}, t)$, function as given by the equation,

$$p(\mathbf{q}, \omega) = \frac{F(\mathbf{q}, \omega)}{1 - \frac{1}{\tau_c} F(\mathbf{q}, \omega)}, \quad (\text{B1})$$

where,

$$F_{ND}(\mathbf{x}, t) = \int \alpha_{ND}(\mathbf{v}) G_{ND}(\mathbf{x}, t, \mathbf{v}) d^N \mathbf{v}. \quad (\text{B2})$$

We wish to verify that,

$$F_{2D}(\mathbf{x}, t) = \int F_{3D}(\mathbf{x}, t) dz. \quad (\text{B3})$$

During the remainder of this proof the 2D side is on the left, and the 3D side is on the right. Writing this in terms of the velocity averaged G functions,

$$\int \alpha_{2D}(v) G_{2D}(\mathbf{x}, t, \mathbf{v}) d^2 \mathbf{v} = \int \int \alpha_{3D}(v) G_{3D}(\mathbf{x}, t, \mathbf{v}) d^3 \mathbf{v} dz, \quad (\text{B4})$$

$$\int \alpha_{2D}(v) \delta^2(\mathbf{x} - \mathbf{v}t) e^{-\frac{t}{\tau_c}} d^2 \mathbf{v} = \int \int \alpha_{3D}(v) \delta^3(\mathbf{x} - \mathbf{v}t) e^{-\frac{t}{\tau_c}} d^3 \mathbf{v} dz. \quad (\text{B5})$$

In polar coordinates we can define the delta function,

$$\delta^2(\mathbf{x}) = \frac{\delta(\rho)}{\rho} \delta(\phi), \quad (\text{B6})$$

where $\rho = \sqrt{x^2 + y^2}$, and $\phi = \arctan(y/x)$. Similarly in spherical coordinates we have,

$$\delta^3(\mathbf{x}) = \frac{\delta(r)}{r^2} \frac{\delta(\theta)}{\sin \theta} \delta(\phi), \quad (\text{B7})$$

with, $r = \sqrt{x^2 + y^2 + z^2}$, $\theta = \arctan(\sqrt{x^2 + y^2}/z)$ and $\phi = \arctan(y/x)$.

Inserting these definitions into equation (B5) and writing the integration over polar and spherical coordinates we have,

$$\int \int \alpha_{2D}(v) \frac{\delta(\rho - vt)}{\rho} \delta(\phi - \phi_v) e^{-\frac{t}{\tau_c}} v dv d\phi_v \quad (\text{B8})$$

$$= \int \int \alpha_{3D}(v) \frac{\delta(r - vt)}{r^2} \frac{\delta(\theta - \theta_v)}{\sin \theta} \delta(\phi - \phi_v) e^{-\frac{t}{\tau_c}} v^2 \sin \theta_v dv d\theta_v d\phi_v dz. \quad (\text{B9})$$

Integration over the angular coordinates in each gives,

$$\int \alpha_{2D}(v_\rho) \frac{\delta(\rho - v_\rho t)}{\rho} e^{-\frac{t}{\tau_c}} v_\rho dv_\rho = \int \int \alpha_{3D}(v) \frac{\delta(r - vt)}{r^2} e^{-\frac{t}{\tau_c}} v^2 dv dz. \quad (\text{B10})$$

We can continue if we assume that z can be determined from r and ρ according to figure 11 by,

$$z = \sqrt{r^2 - \rho^2}. \quad (\text{B11})$$

Therefore if we wish to integrate over z , the definition of a projection, we can change this to in integration over r by,

$$dz = \frac{2r dr}{\sqrt{r^2 - \rho^2}}. \quad (\text{B12})$$

Inserting this into the right hand side in equation (B10),

$$\int \alpha_{2D}(v_\rho) \frac{\delta(\rho - v_\rho t)}{\rho} e^{-\frac{t}{\tau_c}} v_\rho dv_\rho = \int \int_\rho^\infty \alpha_{3D}(v) \frac{\delta(r - vt)}{r^2} e^{-\frac{t}{\tau_c}} v^2 dv \frac{2r dr}{\sqrt{r^2 - \rho^2}}, \quad (\text{B13})$$

$$\int \alpha_{2D}(v_\rho) \frac{\delta(\rho - v_\rho t)}{\rho} e^{-\frac{t}{\tau_c}} v_\rho dv_\rho = \int_0^\infty \alpha_{3D}(v) e^{-\frac{t}{\tau_c}} \frac{2v dv}{t \sqrt{vt^2 - \rho^2}} (1 - \Theta(\rho - vt)). \quad (\text{B14})$$

$\Theta(\rho - vt)$ is the Heaviside step function, it is needed because $r \geq \rho$, and prevents the function from going imaginary. To continue we define a 2D velocity distribution, $\alpha(v_\rho)_{2D}$, as a projection from the 3D velocity distribution according to figure 12. Let us define the 2D velocity distribution as,

$$\alpha_{2D}(v_\rho) = \int_{v_\rho}^\infty \frac{\alpha_{3D}(v) 2v dv}{\sqrt{v^2 - v_\rho^2}}. \quad (\text{B15})$$

Inserting this we have,

$$\int \int_{v_\rho}^\infty \frac{\alpha_{3D}(v)2v dv}{\sqrt{v^2 - v_\rho^2}} \frac{\delta(\rho - v_\rho t)}{\rho} e^{-\frac{t}{\tau_c} v_\rho} dv_\rho = \int_0^\infty \alpha_{3D}(v) e^{-\frac{t}{\tau_c}} \frac{2v dv}{t \sqrt{(vt)^2 - \rho^2}} (1 - \Theta(\rho - vt)). \quad (\text{B16})$$

We continue by scaling the delta function,

$$\int \int_{v_\rho}^\infty \frac{\alpha_{3D}(v)2v dv}{\sqrt{v^2 - v_\rho^2}} \frac{\delta(v_\rho - \frac{\rho}{t})}{t\rho} e^{-\frac{t}{\tau_c} v_\rho} dv_\rho = \int_0^\infty \alpha_{3D}(v) e^{-\frac{t}{\tau_c}} \frac{2v dv}{t \sqrt{(vt)^2 - \rho^2}} (1 - \Theta(\rho - vt)). \quad (\text{B17})$$

Integrating over v_ρ we find,

$$\int_{\frac{\rho}{t}}^\infty \frac{\alpha_{3D}(v)2v dv}{\sqrt{v^2 - (\frac{\rho}{t})^2}} \frac{1}{t\rho} e^{-\frac{t}{\tau_c} \frac{\rho}{t}} \left(1 - \Theta(-\frac{\rho}{t})\right) = \int_0^\infty \alpha_{3D}(v) e^{-\frac{t}{\tau_c}} \frac{2v dv}{t \sqrt{(vt)^2 - \rho^2}} (1 - \Theta(\rho - vt)), \quad (\text{B18})$$

$$\int_{\frac{\rho}{t}}^\infty \frac{\alpha_{3D}(v)2v dv}{t \sqrt{(vt)^2 - \rho^2}} e^{-\frac{t}{\tau_c}} \left(1 - \Theta(-\frac{\rho}{t})\right) = \int_0^\infty \alpha_{3D}(v) e^{-\frac{t}{\tau_c}} \frac{2v dv}{t \sqrt{(vt)^2 - \rho^2}} (1 - \Theta(\rho - vt)). \quad (\text{B19})$$

Again the Heaviside is there to keep the function real. In general we have $v > 0$, and $r \geq \rho$, so we can take the real part of the integral from zero to infinity,

$$\text{Re} \left[\int_0^\infty \frac{\alpha_{3D}(v)2v dv}{t \sqrt{(vt)^2 - \rho^2}} e^{-\frac{t}{\tau_c}} \right] = \text{Re} \left[\int_0^\infty \frac{\alpha_{3D}(v)2v dv}{t \sqrt{(vt)^2 - \rho^2}} e^{-\frac{t}{\tau_c}} \right]. \quad (\text{B20})$$

We have verified that equation (B3) is valid. Therefore with an isotropic velocity distribution we can find the results of the projected 3D random walk with the projected velocity distribution and the 2D random walk. We should point out that this projection is already satisfied by Maxwellian distributions, where we found that the conditional density is the same for 1D, 2D and 3D.

The spectrum of a 3D CTRWT is a projection if the function in question does not depend on one or more of the Cartesian coordinates of the 3D system. Regardless of dimensions used in the model if a function does not depend on a particular Cartesian coordinate

that coordinate can be integrated away. Consider the spectrum of an arbitrary function $h(\rho, \phi, z) = h(\rho, \phi)$ in cylindrical coordinates,

$$\int_{-\infty}^{\infty} h(\rho, \phi) e^{-i\mathbf{q}\cdot\mathbf{x}} d^3\mathbf{x} = H(q_\rho, q_\phi) \delta(q_z). \quad (\text{B21})$$

We have $q_z = 0$ for all z . This is equivalent to integrating over the z direction, and is the definition we used as a projection onto the x, y plane. Thus, when we solve for the Fourier transform we are automatically taking the projection onto the plane normal to the z direction. Therefore isotropic velocity distributions in Cartesian coordinates allows the random walk in $1D$ or $2D$ to solve for the projections of the $3D$ random walk.

REFERENCES

- ¹N. Bloembergen, E. Purcell, and R. Pound, “Relaxation Effects in Nuclear Magnetic Resonance Absorption,” *Physical Review*, vol. 73, no. 7, pp. 679–712, 1948.
- ²R. Golub, R. M. Rohm, and C. M. Swank, “Reexamination of relaxation of spins due to a magnetic field gradient: Identity of the Redfield and Torrey theories,” *Physical Review A*, vol. 83, no. 2, p. 023402, 2011.
- ³G. Pignol, M. Guigue, A. Petukhov, and R. Golub, “Frequency shifts and relaxation rates for spin-1/2 particles moving in electromagnetic fields,” *Physical Review A*, vol. 92, p. 053407, 2015.
- ⁴A. Redfield, “On the theory of relaxation processes,” *IBM Journal*, vol. January, pp. 19–31, 1957.
- ⁵C. P. Slichter, *Principles of Magnetic Resonance. Third Edition*. Springer, 1996.
- ⁶D. D. McGregor, “Transverse relaxation of spin-polarized ^3He gas due to a magnetic field gradient,” *Physical Review A*, vol. 45, no. 5, pp. 2631–2635, 1990.
- ⁷J. M. Pendlebury, W. Heil, Y. Sobolev, P. G. Harris, J. D. Richardson, R. J. Baskin, D. D. Doyle, P. Geltenbort, K. Green, M. G. D. van der Grinten, P. S. Iaydjiev, S. N. Ivanov,

- D. J. R. May, and K. F. Smith, “Geometric-phase-induced false electric dipole moment signals for particles in traps,” *Phys. Rev. A*, vol. 70, p. 032102, Sep 2004.
- ⁸S. K. Lamoreaux and R. Golub, “Detailed discussion of a linear electric field frequency shift induced in confined gases by a magnetic field gradient: Implications for neutron electric-dipole-moment experiments,” *Phys. Rev. A*, vol. 71, p. 032104, Mar 2005.
- ⁹A.K. Petukhov, G. Pignol, D. Jullien, and K.H. Andersen, “Polarized ^3He as a probe for short-range spin-dependent interactions,” *Physical Review Letters*, vol. 105, no. 17, p. 170401(4), 2010.
- ¹⁰S. M. Clayton, “Spin relaxation and linear-in-electric-field frequency shift in an arbitrary, time-independent magnetic field,” *Journal of Magnetic Resonance*, vol. 211, no. 1, pp. 89–95, 2011.
- ¹¹C.M. Swank, A.K. Petukhov and R. Golub, “Correlation functions for restricted brownian motion from the ballistic through to the diffusive regimes,” *Physics Letters A*, vol. 376, no. 34, pp. 2319–2324, 2012.
- ¹²Jaume Masoliver, Josep M. Porra and George H. Weiss, “Some two and three-dimensional persistent random walks,” *Physica A*, vol. 193, pp. 469–482, 1993.
- ¹³R. Burioni, G. Gradenigo, A. Sarracino, A. Vezzani and A. Vulpiani, “Rare events and scaling properties in field induced anomalous dynamics,” *Journal of Statistical Mechanics: Theory and Experiment*, p. P09022, 2013.
- ¹⁴R. Burioni, G. Gradenigo, A. Sarracino, A. Vezzani and A. Vulpiani, “Scaling Properties of Field-Induced Superdiffusion in Continuous Time Random Walks,” *Communications in Theoretical Physics*, vol. 62, no. 4, pp. 514–520, 2014.
- ¹⁵I. Oppenheim and P. Mazur, “Brownian Motion in Systems of Finite Size,” *Physica*, vol. 30, pp. 1833–1845, 1964.
- ¹⁶V. Zaburdaev, S. Denisov, and P. Hanggi, “Space-Time Velocity Correlation Functions for Random Walks,” *Physical Review Letters*, vol. 110, p. 170604, 2013.
- ¹⁷B.H. McGuyer, R. Marsland, III, B.A. Olsen, and W. Happer, “Cusp Kernels for Velocity-Changing Collisions,” *Physical Review Letters*, vol. 108, p. 183202, 2012.

- ¹⁸R.C. Wayne, and R.M. Cotts, “Nuclear-Magnetic-Resonance Study of Self Diffusion in a Bounded Medium,” *Physical Review*, vol. 151, no. 1, pp. 265–272, 1966.
- ¹⁹J.C. Tarczón, W.P. Halperin, “Interpretation of NMR Diffusion Measurements in Uniform and Nonuniform Field Profiles,” *Physical Review B*, vol. 32, p. 2798, 1985.
- ²⁰T. Keyes and Branka Ladanyi, ““Long time tails” in finite systems,” *The Journal of Chemical Physics*, vol. 62, no. 12, pp. 4787–4789, 1975.
- ²¹R.F.A Dib, F Ould-Kaddour, and D. Levesque, “Long-time behavior of the velocity autocorrelation function at low densities and near the critical point of simple fluids,” *Physical Review E*, vol. 74, p. 011202, 2006.
- ²²J. E. Opfer, K. Luszczynski, and R.E. Norberg, “Diffusion Coefficients and Nuclear Magnetic Susceptibility of Dilute ^3He ,” *Physical Review*, vol. 172, pp. 192–198, 1968.
- ²³Guillaume Pignol, Stephanie Rocca, “Electric-dipole-moment-searches: Reexamination of frequency shifts for particles in traps,” *Physical Review A*, vol. 84, no. 4, p. 042105(5), 2011.
- ²⁴Christopher Swank, *An Investigation in the Dynamics of Polarized Helium-3 in Superfluid Helium-4 for the Spallation Neutron Source (SNS) neutron-electric-dipole-moment (nEDM) experiment*. PhD thesis, North Carolina State University, 2012.
- ²⁵K. C. Hasson, G. D. Cates, K. Lerman, P. Bogorad, and W. Happer, “Spin relaxation due to magnetic-field inhomogeneities: Quartic dependence and diffusion-constant measurements,” *Physical Review A*, vol. 41, no. 7, pp. 3672–3688, 1990.
- ²⁶R. Golub and S. K. Lamoreaux, “Neutron electric-dipole moment, ultracold neutrons and polarized ^3He ,” *Physics Reports*, vol. 237, no. 1, pp. 1–62, 1994.
- ²⁷John Wilks, *The Properties of Liquid and Solid Helium*. Oxford, 1967.
- ²⁸S.K. Lamoreaux, et al., “Measurement of the ^3He mass diffusion coefficient in superfluid ^4He over the 0.45-0.95 K temperature range,” *Europhysics Letters*, vol. 58, no. 5, pp. 718–724, 2002.
- ²⁹G. Baym, D.H. Beck and C.J. Pethick, “Transport in ultradilute solutions of ^3He in superfluid ^4He ,” *Physical Review B*, vol. 92, p. 024504, 2015.

- ³⁰A. L. Barabanov, R. Golub and S. K. Lamoreaux, “Electric dipole moment searches: Effect of linear electric field frequency shifts induced in confined gases,” *Physical Review A*, vol. 74, no. 5, p. 052115(11), 2006.
- ³¹M. Abramowitz and I. Stegun, *Handbook of Mathematical Functions*. Dover Publications, 1964.